A Phase Field Crystal Study
of Freezing and Melting

by

Kristin Sæterdal Myhra

Physics of Geological Processes

Thesis submitted for the degree
Master of Science

Department of Physics

Faculty of Mathematics and Natural Sciences

University of Oslo

June 2011

Acknowledgements

Thanks to my amazing supervisor, Luiza Angheluta. Thank you for the great patience you have possessed, for the enthusiasme you have served me when I have been demotivated and for all your help and accessibility. Thanks for everything you have taught me, amongst them that one sometimes just need to have things done. Thank you, Luiza!

Thanks to my fellow students for keeping me on track and for creating an inspiring study environment. I especially want to thank Elvira, Håkon and Øystein for fantastic collaboration during courses and for your friendships. These years had not been the same without Elviras enthusiasme, Håkons steady-state manner through any crisis and Øysteins joy spreading puns. Thanks to Kristin,"the first one", for being the experienced one all through our first year at PGP. Thanks also to the newest contributions to the PGP-master group, Liene and Even, for coping with my bullying and cry for attention.

Thanks to the whole(!) PGP environment for fruitful discussions and open office doors. Both to the geologists for careful explanations of various geological phenomena and to the physisists for challenging me within my own field. Thanks to those of you who have contributed to my thesis through discussions and proof reading and to those of you who have fed me with sweets through the last two years. A great thanks to all of you also for the friendly and social atmosphere in the halls of PGP. An especial thanks to the group of girls, Marta, Kirsten, Jacqueline and Maya for the female touch you bring to the scientific community.

I also have to thank my friends outside of PGP. First of all, thanks to my former study environment back in Bergen for great collaboration and a brilliant social environment through my bachelor degree. A special thanks to my roommates, Åste, Ingvild and Marthe for a lovely appartment atmosphere and for your positive attitudes. Thanks to my friends who fill my freezer with buns and calm me down when I'm all stressed out. Thanks to all of my friends in Oslo and Bergen who keeps me occupied with other activities than studies.

At last I want to thank my parents and my sister. Thanks to my wonderful mum and dad who are always pleased as long as I do my very best. Thanks to my lovely sister, Tone, for being older, calmer and always a step ahead of me.

Contents

Chapter 1

Introduction

1.1 States of matter

The states of matter, and phase transitions from one to another, have been of interest for scientists for decades, and fascinated humans even longer. Progress in understanding the nature of phase transitions has been achieved in experimental work, theoretical work and numerical simulations. Whilst many of such phase transitions are now rather well known, the melting mechanism is still a puzzle.

Through the years, the roles of both dimensionality and impurities have been evaluated in the search for the melting mechanism, but the small scale details of the two dimensional transition is still not fully understood. Disagreement between the theoretical approaches and the experimental results have made it difficult to reveal the mechanism of melting. Without a full understanding of the melting mechanism, it is difficult to predict the critical behaviour of materials in nature, as well as in laboratories.

"Thales of Miletus taught that all things are water" - Aristotle [4]

The first ideas of matter was developed already by the early Greek philosophers. The ancient Greeks were concerned with states of matter even though they lived in a society with no developed science and no pure mathematics [4]. The philosopher Thales is believed to be one of the first to seek for the understanding of the nature of substances. He stated that water is the origin of all matter, that is a definition of "water" which includes all types of matter in the liquid state. By observing liquids, the philosophers realized that the fluid substance could produce all the different states of matter through phase transitions, and hence they argued that liquid had to be a principal element in nature.

Later, natural sciences have taken over the task to classify the different states of matter. As the same set of molecules can create different phases, the state of matter has to be determined by the arrangement of the molecules. Hence, it is reasonable to define the solid and liquid states in terms of how their molecules are organized.

In a perfect crystalline solid, the molecules are bound in periodic lattices creating a rigid structure. At the absolute zero temperature, all atoms are in equilibrium, and there is no movement in the system. As the temperature increases, the energy in the system cause the atoms to move, but as long as the movement is restricted to vibrations around the confined lattice position, the solid will remain rigid. At some critical energy, which we percieve as temperature, the rigid structure of the solid breaks down. Then, in the limit of low density, the molecules can move around freely, only restricted by the external boundaries of the system, e.g. the container in which the fluid flows. This is the perfect liquid phase, a disordered phase in which the system is homogeneous with randomly distributed molecules.
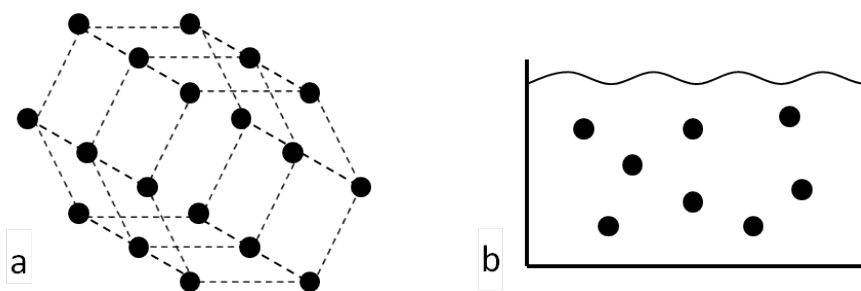

Figure 1.1: (a) Illustration of the perfect solid state. The atoms are locked in their positions and the matter retains it shape and volume. The only motion in the system are the lattice vibrations. (b) Illustration of the perfect liquid state. The molecules move freely within the system. The atoms collide with each other in the system and hence frictional force is induced.

Even though the definitions of the two perfect phases seem quite understandable, a phase transition between them is more perplex. Changes of state are of the most dramatic and fascinating phenomena exhibited by condensed matter, and the process of melting is especially confusing [8]. As the different states of matter are determined by the collective behaviour of the molecules in the system, it is reasonable to expect that the laws of physics are capable of predicting the behaviour of the system through a phase transition. The search for universalities in the melting mechanism, i.e. the solid-liquid phase transition, have been particularly challenging and various theories have been developed. We emphasize in particular the Kosterlitz-Thouless-Halperin-Nelson-Young-theory, the KTHNY-theory, [18, 39], and the grain-boundary-theory, [7], but neither of the developed theories seem to be able to capture the wide variety in the experimental result.

Theoretically, we comprehend phase transitions through the laws of thermodynamics, by means of the energy in the system. The appearance of different phases is dependent on state variables, such as temperature and density in the system. In Ref. [20], Löwen boils it down to a fundamental question;

"What kind of phases occur for a given interaction potential as a function

of the thermodynamical parameters, temperature, T, and density, ρ?"

That is, the search for a general understanding of phase transitions and their universalities is a search for how the structure of a material changes with variating state variables. By revealing such universalities, we can predict how and when different materials loose their resistance to external stresses.

1.2   A fascinating phenomenon

So far, we have argued that a phase transition is a change of state of matter which alter the nature of substances. Phase transitions are important in all condensed matter physics and is hence of interest in science as well as in industry. As an example, the development of new materials within material sciences, are based on the increasing knowledge about formation and changes of microstructures [31].

As common phenomena in nature, phase transitions are important for various fields within natural sciences. The importance of phase transitions within the field of geology was discovered more than 2000 years ago by the Greek scientist Strabo, who observed that magma from a volcanic eruption cooled down and solidified on the surface of the Earth [16]. Since then, the knowledge about geological systems have improved significantly. It is now well known that the high temperature, and pressure, differences between the Earth's surface and its interior cause incessant transitions between solid rocks and viscous magma, though on a geological time scale. The last couple of years, geophysics have improved further through increasing knowledge about mineral physics [26]. Many of the geological forms we observe in nature are caused by different minerals crystallizing under various conditions. Due to natural impacts, such as impurities and external forces, the resulting patterns can be very fascinating, as well as quite difficult to describe. Also other natural phenomena are dependent on phase transitions, e.g. glaciers which require specific weather conditions over time in order to persist. That is, the existance of glaciers is dependent on a positive mass balance, that is the balance between the mass of ice freezing during winter and the mass which melts during summer. Frost at your window and freezing lakes are two typical two dimensional phase transitions. The first being crystal growth on an undercooled window substrate, the latter being crystallization process in the liquid-air interface.

The difference between the rigid solid phase and the mobile liquid phase play an important role in daily life. One can not undermine the importance of the melting transition when you go for skiing and a liquid-like layer on top of the snow acts as a mobile substance at which your skies can slide. Neither of the freezing process high in the Earth's atmosphere which forms the snowflakes you ski on. Hence, your skiing activity is dependent on two phase transitions, that is freezing of snow crystals and the subsequent surface melting which ensures that your skies glide on the crystalline snow. During summer, when the seasonal changes no longer encourages skiing, one

can not deny the importance of the phase transition which causes cream and melted chocolate to transform into ice cream.

1.3   The search for the melting mechanism

As previously mentioned, the search for universalities of the melting mechanism have been puzzle for theoretical scientists since the nineteenth century. The observation of mild changes in physical parameters, such as volume and specific heat, through the melting process suggested a melting transition with gradual change of matter properties within the same state, i.e. a continuous melting transition, more than a transition between two different states. The idea of temperature dependent thermal vibrations in lattice structures led to an idea of increasing atomic vibrations being the mechanism of melting. An early scientific proposal was by Fredrick Lindemann in 1910, [25], who obtained a rather simple estimate of the melting temperature by a connection to atomic vibrations. The well known Lindemann theory appears to be the first adoption of quantum theory applied to condensed matter, after Einstein's proposal in 1907 [8]. The vibrational approach is based on the assumption that at a certain critical temperature, the molecules acquire enough energy to break the bonds in the structure. Hence the molecules are no longer confined in their positions, and "the crystal has shaken it self to pieces" [14].

The vibrational approach did not succeed in revealing the mechanism of melting and the search continued. As the most striking difference between the solid and the liquid phases is the degree of order, it seemed reasonable that lattice dimensionality and the possibility of defects, such as dislocations, in the lattice played an important role in the process of melting.

That is, the attention was drawn to the effect of dimensionality in an early stage in the search of the melting scenario with Peierls as one of the originators [9]. He studied the positional order of lower dimensional crystals for temperatures above the absolute zero. An one-dimensional crystal was modeled as a simple chain of identical particles with regular distances, a system in which the long-range order can not persist for temperatures above the absolute zero. Thus, the crystal structure does not really exist for any thermal motion. In contrast, in a three-dimensional crystalline material, the long-range order persists for increasing thermal motion until a well defined critical point where a dicontinuous phase transition takes place.

The two-dimensional situation is the borderline between the 3D long-range order and 1D nonexistent order, and the melting transition in this dimension is still a puzzle. As the temperature increases the particles are displaced relative to their equilibrium positions. Peierls predicted a gradual destroyed long rang order and thus a transition without a well defined critical point. His prediction was later dismissed as misleading and the search for the theory of the 2D melting transition continued [8].

The lack of understanding of the transition in two dimensions stimulated the development of 2D models of matter and the study of the physics of them [8]. In

addition to the role of dimensionality, the effect of impurities in the system was investigated by the scientists. In nature, perfect materials are not likely to exist. Hence, condensed matter, and crystals therein, are arrangements of particles in which defects is likely to be present. The presence of defects will disturbe the geometry of the material structure, and thus also the dynamics of the crystal structure [17]. In 1952, Shockley proposed a definition of liquid to be a solid so densly packed with dislocations that is gets a viscous behaviour, [26], and calculated the fluid viscosity by means of the movement of dislocations in the material. Hence, the response to external stresses can possibly be described by the way dislocations are generated and move through the crystal.

In addition to natural impurities, also the crystal surface and internal grain boundaries act as defects in the material. The former represents the boundary between the crystal and its surroundings. Along this boundary, the solid is at its weakest and the thermal energy can most easily disorder the structure. Hence, the boundary plays the role of the most important defect in the system [9]. The later represents the boundaries between crystals of different lattice orientations in a polycrystalline material. These are defined as chains of defects and play the role of surface defects for each of the grains in the crystalline network. The prescence of defects in a material weakens the structure and can hence mediate the melting process [17]. That is, the material might stat to melt from these defects before the bulk of the system reaches the critical melting temperature of the material. Hence, the presence of defects may mediate a premelting phenomena.

1.4 Summary of the thesis

Though melting is a common phase transition in nature, the small scall details of the crystal breakdown in two dimensions are not yet fully understood. In this thesis we will present a numerical investigation of melting and freezing in two dimensions through the phase field crystal model. We start out, in the second chapter, by discussing phase transitions by means of disorder-order transitions through the phase field method. The method is suitable of describing phase transitions in heterogeneous and isotropic systems and is an important tool for modeling microstructural evolution [38]. We continue in the third chapter by deriving the phase field crystal method. That is a method in which the isotropic approximation is relaxed and the free energy functional is constructed to ensure a periodic structure in the equilibrium state. By this approach, important features such as crystal orientation, defects and deformations are naturally incorporated in the model. Hence, this method provides a suitable method for describing the process of crystal growth as well as the breakdown of the crystalline structure, that is the processes of freezing and melting respectively. Additionaly, a set of amplitude equations are presented for the study of the dynamical evolution in the crystalline phase.

In the fourth chapter, we discuss the process of melting and the role of dimension-

ality and dislocations in the phase transition. We limit our work to two dimensional systems and investigate the evolution of melting numerically with a particular focus on the role of defects in the phase transition. The simulated melting is induced by two different protocols, that is uniform heating and applied shear stress, and we evaluate our numerical results relative to the theory of dislocation mediated melting. In the fifth, and last, chapter we summarize our results and elaborate upon the challenges in the search for the melting mechanism. As a closure, we propose ideas for future work which can be carried through with the phase field crystal method.

Chapter 2

Phase field modeling

In this section we develop simple physical pictures of the dynamics of phase transitions in the mean field approximation. We review the phase field method which is a suitable model for describing phase transitions in heterogenous and isotropic systems, i.e liquid-like systems. In this method the interface between different phases is treated diffusively. The method is based on defining a space and time dependent order parameter which can distinguish between the different phases, hence the rate of change of the order parameter provides a description of the kinetics of the system. The state of a physical system can be characterized by a set of physical quantities, such as density, temperature or concentration. The physical quantities can be both conserved or non-conserved through the transition, and it can relax to a homogeneous and isotropic value (liquid-like phase) or an anisotropic, periodic structure (crystal-like phase). In this section we will investigate the dynamics of phase separation and growth, for physical systems of both non-conserved and conserved field parameters.

2.1   The phase field technique

The kinetics of a phase transition, i.e. the evolution dynamics of a thermodynamically unstable system as it relaxes towards equilibrium has been intensively studied [28]. Phase transitions occur spontaneously in almost all systems which are driven out of their equilibrium state by rapid changes in system parameters, and is hence an important aspect of material science. The field of material science is wide and, in general, separated in 'subfields' dependent on the level of description. From a macroscopic point of view, the phase transition from a liquid to a solid state is recognized through the apperance of a shear resistent crystalline material. The classical approach for treating this transition is dividing the system into two parts. The first being the solid state and the second being the liquid state. The boundary between the two phases is represented by a sharp interface at which the material parameters change discontinously, like a step function. The solidification process then appears as a moving boundary process in which the position of the boundary describes the growth pro-

cess. From a mathematical point of view, this model is simple and tractable. In a numerical implementation,however, the sharp interface method requires tracking of the interfacial position as the transition evolves and hence the model can be numerically challenging [31]. A different approach is the phase field model which is based on the concept of a diffusive interface. In this model, the interface is defined as a narrow region in which the material parameters change continuously. Hence, there is made no distinction between the solid, the liquid and the interface, and the diffusive change in a material parameter across the interface is described through an auxiliary variable. That is, a space and time dependent order parameter, which provides a basis for describing the kinetics in the system. By defining the order parameter to minimize the free energy in stable phases, thermodynamical stability is ensured. The order parameter is kept uniform and constant within stable phases, while it changes continuously across interfaces. Its value indicates different phases and the boundary between two phases need not be tracked as in the classical sharp interface approach. Thus, the phase field technique provides a good numerical tool for predicting the kinetics through a phase transition in heterogeneous and isotropic systems [36]. The material parameters can be both conserved or non-conserved quantities, presented by Cahn-Hilliard equation, or the Ginzburg-Landau equation, respectively.

In Fig.(2.1) we illustrate the interfacial region between two species in a heterogeneous binary system represented by the two approaches discussed above. (a) and (b) depict the sharp and the diffusive interface representation, respectively.
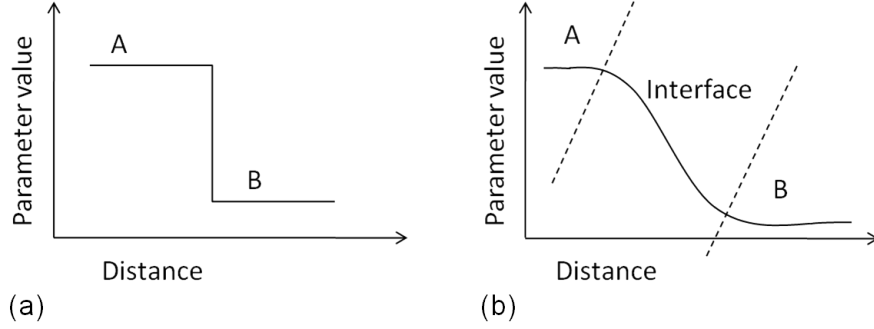
Figure 2.1: Illustration of the interfacial region in a hetereogeneous system consisting of two species, A and B, with different densities. (a) illustrates a system in which the different species are separated by a sharp interface while (b) illustrates a diffusive interface with a continously changing parameter value through a narrow interfacial region

Phase field modeling is one of the fastest growing areas in computational material science and several phase field model approaches have been developed [31]. Here we adopt one of them, a so-called variational approach, based on a thermodynamical treatment of a single scalar parameter. The phase field method results in a set of partial differential equations which will be discussed in the following sections.

2.2 The dynamics of a phase transition

Consider a disordered binary system, i.e. a mixture of two species in a homogeneous state in which the two species are characterized by different densities. A suitable order parameter to describe this system is the density difference between the two species. For temperatures above a critical temperature, T_c, the system admits a single equilibrium phase in which the species appears in a homogeneous mixture, whereas below T_c, there is a degenerated equilibrium with two possible states. The two density fields have different equilibrium patches distributed randomly in space. Hence, a system quenched below T_c will undergo a gradual process of domain coarsening, exhibited by a heterogeneous density field.

Such a system is most easily treated through a mean field approximation of the order parameter. The basis of the mean field approximation is to ignore all spatial fluctuations in the system. Hence, the free energy can be expressed as an analytical function of the order parameter, $\psi(\mathbf{r})$, which can be written as a Taylor expansion. The Landau free energy density provides such a free energy expression of the simple form, [37],

$$f = f_0 + \frac{\alpha}{2}\psi^2(\mathbf{r}) + \frac{1}{4}\psi^4(\mathbf{r}), \tag{2.1}$$

where $\mathbf{r}$ represents the position and $\alpha = (T - T_c)/T_c$ and denotes the undercooling

parameter, i.e the depth of the temperature quench.

The total free energy is obtained by a volume average of the energy density, and the equilibrium energy configuration corresponds to the minimum of the free energy function. That is,

$$\frac{d\mathcal{F}\{\psi\}}{d\psi} = 0$$
$$\alpha\psi + \psi^3 = 0, \tag{2.2}$$

which corresponds to the variational of the free energy in Eq.(2.1). From Eq.(2.2), we see that the sign of α determines the number of equilibrium solutions. For $\alpha > 0$ and $\alpha = 0$ the only equilibrium solution is the trivial $\psi_0 = 0$. On the contrary, for $\alpha < 0$ the system admits two additional solutions at $\psi_{0(1,2)} = \pm\sqrt{-\alpha}$ and hence there are three possible equilibrium states. Fig.(2.2) illustrates the energy landscapes given by the Landau free energy for three different values of α, that is $\alpha > 0$, $\alpha = 0$ and $\alpha < 0$. The equilibrium solutions of Eq.(2.2) are recognized as maxima and minima in the energylandcapes.
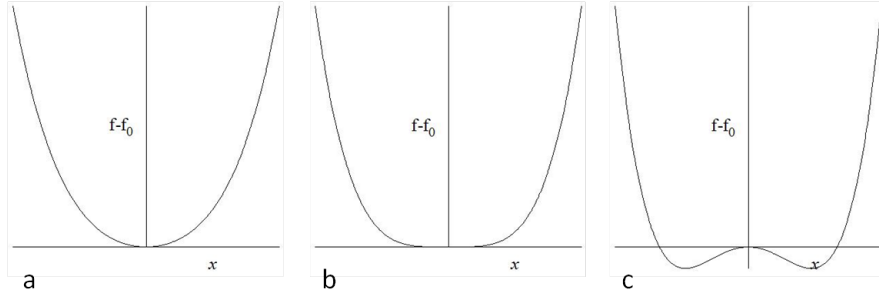

Figure 2.2: Sketch of the energy landscape given by the Landau free energy for decreasing values of α, (a) $\alpha > 0$, (b) $\alpha = 0$ and (c) $\alpha < 0$. For temperatures below the critical, the energy landscape appears as a symmetrical double well potential. For subcritical temperatures, the depth of the wells is controlled by the depth of the temperature quench. A deeper quench leads to deeper 'valleys' and hence one can expect a more rapid phase transition

Below the critical temperature, $\alpha < 0$, we obtain the generic double-well potential and observe that the solutions, $\psi_{0(1,2)} = \pm\sqrt{\alpha}$, are located in the "valleys", bridged by a "hill" at $\psi_0 = 0$ in the energy landscape. This correponds to having two stable equilibria in the valleys and one unstable equilibrium on the hill. Moreover, in the absence of a cubic term in the free energy, we notice that the equilibrium states correspond to exactly the same values in the free energy (symmetric valleys), hence the equilibrium is degenerated. Dynamically, this equilibrium degeneracy implies that when the system is rapidly quenched below the critical temperature, the homogeneous state is no longer the preferred equilibrium state and the system spontaneously

nucleates and grows new equilibrium patches that form domains. The domains are characterized by a lengthscale, $L(t)$, and separated by a diffuse interface, where there are sharp gradients in the density variations.

In the next two subsections, we discuss the dynamics of the system after a temperature quench which results in new equilibrium patches and formation of domains for both non-conserved and conserved fields.

2.2.1 Non-conserved fields

If the two species in the system described in the previous paragraph are competative, that is if a phase grows or shrinks at the expense of the other, the density field is typically non-conserved. The system can be described by a density order parameter, $\psi(\mathbf{r}, t)$, at position $\mathbf{r}$ and time t. In the Ginzburg-Landau theory, the effect of fluctuations is added to the mean field free energy by an additional energy cost associated with heterogeneities near interfaces, hence the free energy is modified by adding a nonlocal term given as

$$\mathcal{F}\{\psi\} = \int dv \left(f(\psi) + \frac{\kappa}{2}|\nabla\psi|^2 \right), \tag{2.3}$$

where $f(\psi)$ is the local energy contribution described by the double-well potential in the previous section. The second term is an additional non-linear contribution corresponding to the energy increase near interfaces. The new equilibrium configuration corresponds to the minimum of this global free energy, which can be expressed as

$$\frac{\delta\mathcal{F}}{\delta\psi} = \alpha\psi + \psi^3 - \kappa\nabla^2\psi = 0. \tag{2.4}$$

The trivial solution to this system is the $\psi_0 = 0$ solution. For a flat interface, that is a 1D approximation, the problem of solving Eq.(2.4) reduces to only one direction, that is the one across the interface. Hence, the gradient term reduces, $\nabla^2\psi \to \frac{d^2\psi}{dx^2}$, and it is possible to obtain the additional non-trivial solutions analytically. Suppose the interface is stretched along the y-direction. Then, after one integration, Eq. (2.4) for the density profile in the perpendicular direction along the x-axis simplifies to

$$\kappa\frac{d^2\psi}{dx^2} = \alpha\psi + \psi^3. \tag{2.5}$$

This can be reduced to a first order differential equation,

$$\frac{d\psi}{dx} = \sqrt{\frac{2\alpha\psi^2 + \psi^4 + c}{2\kappa}}, \tag{2.6}$$

where c denotes the constant of integration. Keep in mind that in order for the system to admit to a degenerated equilibrium with two states, then $\alpha < 0$. The interfacial

profile between these two states is given by the solution of Eq.(2.6). As the phase gradients across the interface vanish in the equilibrium bulks, the rhs of Eq.(2.6) equals zero in these states, that is for $\psi_{0(1,2)} = \pm\sqrt{-\alpha}$. By substitution we obtain an expression for the constant of integration, c, given by,

$$\psi_0^4 + 2\alpha\psi_0^2 + c = 0 \quad \Rightarrow c = \alpha^2. \tag{2.7}$$

Now, Eq.(2.6) reduces to

$$\frac{d\psi}{dx} = \frac{\alpha + \psi^2}{\sqrt{2\kappa}}, \tag{2.8}$$

with solution

$$\psi(x) = \sqrt{-\alpha}\tanh\left(\sqrt{\frac{-\alpha}{2\kappa}}x\right). \tag{2.9}$$

Hence, we have obtained an expression for the interfacial profile between the two equilibrium states.

The dynamics of the relaxtion towards a new equilibrium state can be described by the Ginzberg-Landau equation with $\frac{\delta\mathcal{F}}{\delta\psi}$ from Eq.(2.4),

$$\frac{\partial\psi(\mathbf{r}, t)}{\partial t} = -\frac{\delta\mathcal{F}}{\delta\psi}$$
$$\frac{\partial\psi(\mathbf{r}, t)}{\partial t} = -\alpha\psi(\mathbf{r}, t) - \psi^3(\mathbf{r}, t) + \kappa\nabla^2\psi(\mathbf{r}, t). \tag{2.10}$$

The evolution towards a segregated phase for a non-conserved density field can be investigated by solving the Ginzberg-Landau equation, Eq.(2.10), numerically. In Fig.(2.3), we depict the evolution of the density field as it reorganizes into domains after a temperature quench. The random initial condition is embossed by large amount of interfaces throughout the system. Due to the energy cost of having interfacial profiles, the system reorganizes in order to reduce the interfacial length in the system. The two components demix into a gradually increasing heterogeneous state of coarser domains.
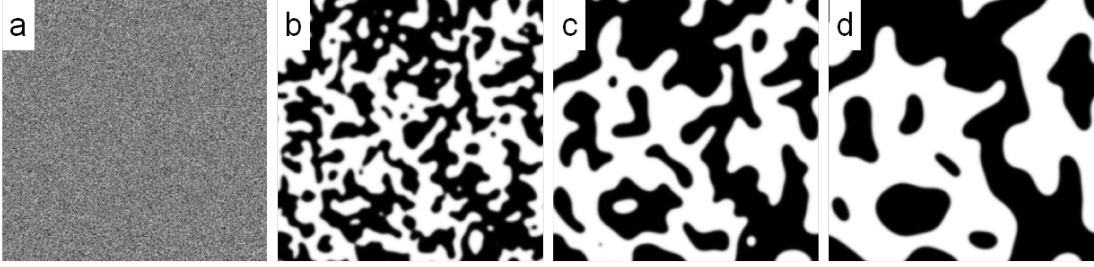
Figure 2.3: Snapshots of the temporal evolution of a quenched system with a non-conserved density field. (a), (b), (c) and (d) represent the initial random start, and three successive later times. The initial homogeneous system reorganizes into a more heterogeneous state consisting of domains with different densities. In the steady state, the interface and the domains possess different local equilibria. Undercooling parameter and mean density $\alpha = -1$ and $\psi_0 = 0$. System size nx=ny=500.

The coarsening regime of the path towards a new equilibrium is characterized by domains growing with length scale, $L(t)$. In non-conserved systems, the domain scaling obeys the Lifshitz-Allen-Cahn-law, the LAC-law, [28],

$$L(t) = \sqrt{t}, \tag{2.11}$$

where $L(t)$ denotes the time dependent length scale. The LAC-law implies that the growth slows down with time.

A feature of the new equilibrium state is an equilibrium interface profile separating the two domains, each in its equilibrium state with constant density. In the 1D approximation, this interfacial profile is represented by the non-trivial analytical solution given in Eq.(2.9). In Fig.(2.4), a comparison between the analytical and numerical interfacial density profile is made for different quenching depths.
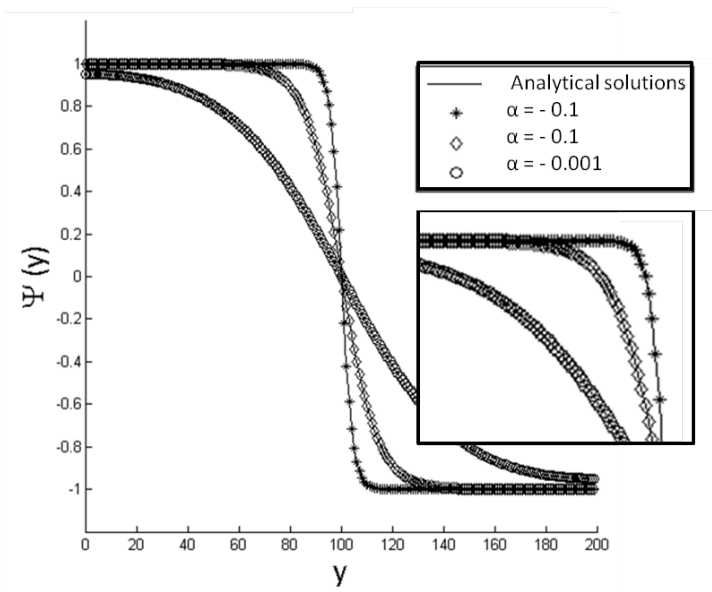
Figure 2.4: The figure illustrates a comparison of the numerical and analytical non-trivial solutions for the flat interface profile when the system is quenched at different temperatures. The solid lines represent the analytical solutions, whilst the dots represent the different numerical solutions. α denotes the undercooling parameter $\alpha = (T - T_c)/T_c$ and hence gives a description of the quenching depth. Deeper quenches require larger gradients across the interface and hence lead to sharper interfacial profiles. The analytical and numerical profiles are in agreement.

The interfacial profiles vary with respect to the quenching depth. Deeper quenches correspond to systems driven further from their initial equilibrium state. Hence the temperature gradients across the interface are larger, resulting in larger interfacial gradients. The interfacial profile is thereby sharper for higher values of the undercooling parameter, α. Less dramatic temperature drops require smaller gradients and hence the interfacial profile appears as more diffuse.

Growth

The growth mechanics of a single droplet in a binary system can be evaluated by the same differential equation as the separation process. The system is comparable to binary liquid systems which do not mix up well, such as a droplet of vinegar in water. After a temperature quench, the droplet grows or shrinks at the expense of the surrounding liquid and the boundary between the two phases is moving radially. As the droplet grows, its surface area, and thus also the surface energy in the system, increases. The rate of growth can be connected to the rate of the free energy and it can be shown that the mean curvature is directly proportional to the growth velocity. Hence, the direction of the moving boundary is dependent on the surface energy of

the blob, represented by the curvature of the blob.

The process of a single droplet growing isotropically is illustrated in Fig. 2.5
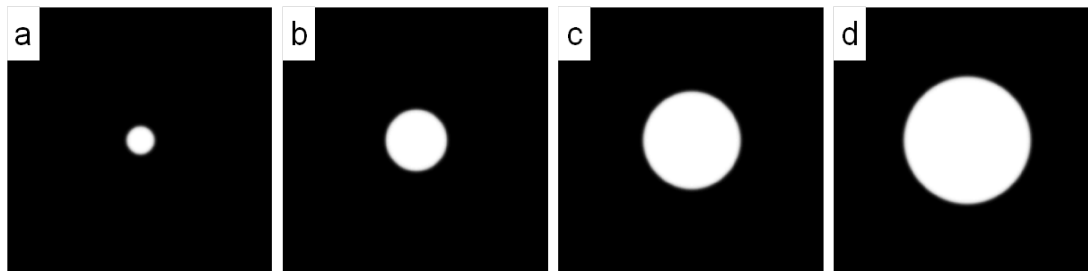
Figure 2.5: Pictures (a)-(d) illustrate isotropic growth at successive time steps. An initial droplet grows radially outwards after a rapid temperature drop. The droplet grows at the expense of the surrounding liquid, hence the growth evolution is governed by the Ginzberg-Landau equation. Undercooling parameter and mean density $\alpha = -0.25$ and $\psi_0 = 0.25$. System size nx=ny=500.

The growth of the droplet can be calculated by expanding around the planar solution and represented in terms of the droplet radius. In Fig.(2.6) the time development of the droplet radius for different quench depths are plotted together with the rate of growth for the same quench depths. As for the process of phase separation, the droplet growth is dependent on the depth of the temperature quench, i.e. the value of the undercooling parameter. A deep quench drives the system further from its original equilibrium and results in deeper wells of the energy potential represented by Landau free energy, Eq.(2.1). Hence, the gradients in the system are larger and the growth rate is higher than for more shallow quenches.

Figure 2.6: Plot of the time development of the radius of an isotropic growing droplet for different tempreature quenching depths. The inset figure gives the rate of growth for th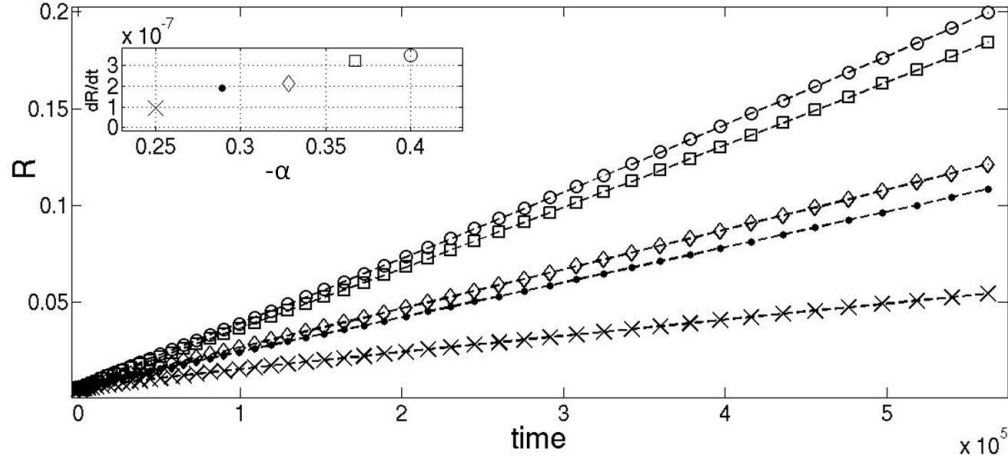e different undercooling parameters, $\alpha = -0.25, -0.289, -0.328 - 0.367, -0.4$. R denotes the radius of the droplet and is normalized with respect to the system size.

2.2.2 Conserved fields

In systems where the parameter fields are conserved, there is no competition between the species in the system. The ordering process is evolving by two species interchanging their positions. Hence, and in contrast to the non-conserved scenario, an evolving phase is now dependent on two process happening simultaneously within the same system. When one specie reorganizes, it is dependent on an other specie to perform the opposite movement simultaneously. Analogous to the Ising model, this process is equivalent to a spin-exchanging process. When one spin flips from +1 to -1 in one part of the system, an other spin must flip simultaneously from -1 to +1 in order to conserve the number of spins. Due to this additional conservation constraint, the dynamics of this system is typically slower than for the non-conserved case.

   In this section, the disordered binary system from the previous section is evaluated in a scenario where the density field is conserved throughout the phase separation. Though the phase separation processes in the non-conserved and conserved cases evolve differently, the same space and time-dependent order parameter, $\psi(\mathbf{r}, t)$, can be used to describe the evolutions of their parameter fields. The additional conservation constraint on the parameter field implies that the order parameter obeys a continuity equation of the form

$$\partial_t \psi(\mathbf{r}, t) + \nabla \cdot J(\mathbf{r}, t) = 0, \tag{2.12}$$

where $J(\mathbf{r}, t)$ denotes the density current through the material. The current has its origin due to flucutations in the density field and hence it can be represented as

$$
\begin{aligned}
J(\mathbf{r},t) &= -m\nabla\mu(\mathbf{r},t) \\
J(\mathbf{r},t) &= -m\nabla\frac{\delta\mathcal{F}\{\psi(\mathbf{r},t)\}}{\delta\psi(\mathbf{r},t)},
\end{aligned}
\tag{2.13}
$$

where $\mu(\mathbf{r},t)$ is the chemical potential and m denotes constant mobility in the medium.

The system is treated in the mean field approximation with local free energy as described by Landau, Eq.(2.1). The energy cost due to hetereogeneities close to the interface is accounted for by an additional non local term. Hence, the global free energy $\mathcal{F}$ is given by Eq.(2.3) with equilibrium configuration

$$
\frac{\delta\mathcal{F}}{\delta\psi} = \psi^3 + \alpha\psi - \kappa\nabla^2\psi = 0.
\tag{2.14}
$$

An equation describing the dynamics of the phase separation process can be obtained by combining the additional conservation constraint, represented by the continuity equation Eq.(2.12), with the minimized free energy functional, Eq.(2.14). The resulting differential equation known also as the Cahn-Hilliard equation, [6, 5], is

$$
\frac{\partial\psi(\mathbf{r},t)}{\partial t} = m\nabla^2\left(\alpha\psi(\mathbf{r},t) + \psi^3(\mathbf{r},t) - \kappa\nabla^2\psi(\mathbf{r},t)\right).
\tag{2.15}
$$

The Cahn-Hilliard equation provides a description of the relaxation process towards a new equilibrium state for a conserved density field, equivalent to the Ginzburg-Landau equation, Eq.(2.10), for the non-conserved density field. If the homogeneous binary system is quenched below the critical temperature, the homogeneous stare is no longer the preferred equilibrium state and hence the system will relax towards a new equilibirum state. The new equilibrium patches form domains and the system undergoes a process in which the two species are segregated into separate areas. Solving Eq.(2.15) numerically, we obtain a description of the phase separation process. In Fig.(2.7), snapshots of the coarsening process at successive timesteps are presented.
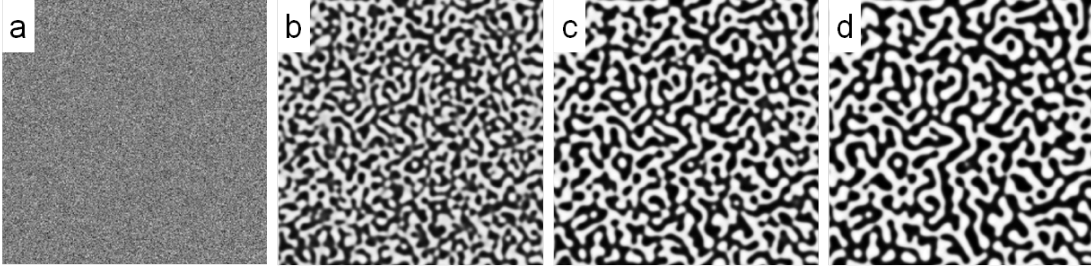
Figure 2.7: Snapshots of the temporal evolution of a quenched system with a conserved density field. (a), (b), (c) and (d) represent the initial random start, and three successive later times. The initial homogeneous system reorganizes into a more heterogeneous state consisting of domains with different densities. In the steady state, the interface and the domains possess different local equilibria. Undercooling parameter and mean density $\alpha = -1$ and $\psi_0 = 0$. System size $nx = ny = 500$.

Also in this system the phase separation process is characterized by a domain length scale, L(t). Due to the additional conservation constraint, the growth is expected to be slower than for the scenario with the non-conserved density field. Lifshitz and Slyozov derived a power law behavior for the temporal evolution of the typical domain scale, [28],

$$L(t) = \sqrt[3]{t}. \tag{2.16}$$

In this section we have discussed modeling of phases in the isotropic approximation, that is in systems where the order parameter is confined across the boundaries, while it relaxes to a certain homogeneous value inside each phase. The phase field method is suitable for isotropic and heterogeneous systems and has been used widely within several fields for many years. Such systems are somewhat idealized physical systems in which natural impurities, such as defects, are not included.

According to Puri, [28], phase separations are typically mediated by vacancies in the system. Hence, impurities do not only act as complications in the system, but might be important contributers to the nature of the phase transition. In the following chapter the phase field crystal model is rigorously derived from the microscopic interactions between colloidal particles. Hence, the periodic nature of the atomic density in the solid is included and defects in the material can be incorporated in the investigation of phase transitions.

Chapter 3

Phase field crystal modeling

In the previous chapter, we discussed modeling of binary liquids or amorphous-like phases. The phase field method has become an important tool for modeling microstructural evolution in material science, [38], but is limited to systems in which the density field of each phase relaxes to a homogeneous and isotropic value at equilibrium. The approximation is suitable for isotropic materials, but can not, for instance, capture the periodic structure of a crystalline material. Thus, it can not easily incorporate important features such as crystal orientation, defects and deformations.

In this chapter, we present the phase field crystal method, as an extension of the classical phase field method, in which the isotropic approximation is relaxed. The method is able to model a system with crystal lattice anisotropy by representing the crystalline phase by a periodic density field. As the method is able to incorporate defects in the periodic structure, it provides a firm basis for modeling imperfect solid materials. Here, we provide a derivation of this model from the microscopic interactions between colloidal particles, based on the paper by van. Teeffelen et al. in Ref. [35]. In addition, we study the dynamical evolution in the crystal phase by means of the amplitude equations, as discussed in Ref. [1, 38]. The steps in the derivation of these equations are presented and their applicability to modeling freezing and melting in crystal and polycrystalline materials is discussed.

3.1   The phase field crystal approach

The process of formation of microstructural materials involves a wide range of length scales, from the atomistic structure to the macroscopic properties of materials. Both the PF-method and the PFC-method possess descriptions of such material processing phenomena by providing a link between microscopic and mesoscopic descriptions of phenomena through modeling the collective behavior of particles on diffusive time scales [13]. The PF-method incorporates the range of scales, but operates with density fields which are homogeneous in space, and hence it fails to incorporate defects and elastic properties [15]. In Ref. [12], Elder et al. proposed a phase field crystal

method as a phenomenological model that incorporates crystal anisotropy. Hence, the model provides a suitable method to describe the process of crystal growth and crystal deformation. As previously discussed, the free energy functional provides a basis of the thermodynamics in a system. Thus, it is convenient to connect the free energy to the parameter field of interest when we want to investigate the evolution of the parameter field through a phase transition. Equivalent to the PF-method, the PFC-method describes the free energy in the system in terms of the density function, $\rho(\mathbf{r}, t)$. However, whilst the density field was uniform in all phases at equilibrium in the PF-method, the density function is now constructed to have the same symmetry as a given crystalline lattice, [11]. That is, in the PFC-method the free energy functional is constructed in the simplest form that produces periodic phase fields in equilibrium. In a liquid phase, the density field relaxes to a homogeneous value, while it is represented by periodic density waves in a crystalline phase. The evolution of these waves can be represented by amplitude equations. The dynamical equation of motion for the density field is chosen to conserve the density field through a phase transition [12]. Hence the PFC-model provides a conserving analogue to the Swift-Hohenberg equation, [1], which treats the atomic structure in systems with non-conserved physical fields. A free energy functional which is minimized by a periodic field includes, in addition to the internal energy, the elastic energy and symmetry properties of the periodic field [11]. Thus, the PFC-method has the ability to describe crystalline materials and thereby incorporate defects, such as dislocations and grain boundaries.

In the following sections we will present the derivation of the equations in the phase field crystal model based on the paper by van Teeffelen et al., [35]. We start by investigating equations of motion for a collection of colloidal particles in an overdamped physical system. Thereafter we derive the Smoluchowski equation from the Langevin equation and specify a free energy functional which minimize to a periodic structure. The equations of motion derived from the variational of the free energy, provide a theoretical basis for the equations of motion in the phase field crystal model, [35], and the relationship between them will be examined. In addition, we derive suitable amplitude equations which posit a description of motion for the periodic density waves in the crystalline structure.

3.1.1   The Langevin equation

Consider a simple physical system in which colloids move through a liquid phase. Each of the colloids follow its own path and, as they move, they bump into the surrounding fluid particles. These collisions induce frictional force in the system and hence the dynamics of the flowing colloids change. In the absence of potential interactions between the colloids, the particles move only due to the random kicks. Hence, the path of a moving colloid is equivalent to the one for a Brownian particle in a force field and the colloids in the system describe random walk.

At the microscale the density field, $\rho(\mathbf{r}, t)$, in a physical system consists of a collection of N colloidal particles in a viscous suspension. As the particles bump into the surrounding fluid, they interact with the fluid particles via a linear viscous drag due to friction. Hence, the density field can be interpreted as a probability density of having a particle at position $\mathbf{r}$ and time t. In such a system, the particle position can be described through the Langevin equation for overdamped particles,

$$\gamma \frac{d\mathbf{r}_i}{dt} = \mathbf{F}_i + \mathbf{f}_i. \tag{3.1}$$

The left hand side denotes the time evolution of each of the colloidal positions $\{\mathbf{r}\} = \{\mathbf{r}_1 \cdots \mathbf{r}_N\}$ and represents the drag force with a friction coefficient, γ. The first term on the right hand side represents a deterministic force induced by the interaction between the colloidal particles, while the second term represents stochastic forces due to random collisions between the colloids in the system. The deterministic interaction between the colloidal particles is given by pairwise additive potentials $u(|\mathbf{r}_i - \mathbf{r}_j|)$. Hence the deterministic force acting on particle i is represented by

$$
\begin{aligned}
\mathbf{F}_i(\{\mathbf{r}\}, t) &= -\nabla_i U(\{\mathbf{r}\}) \\
&= -\nabla_i \left(\frac{1}{2} \sum_{i \neq j} u(|\mathbf{r}_i - \mathbf{r}_j|) \right).
\end{aligned}
\tag{3.2}
$$

The force is determined by the gradient of the interaction potential $U(\{\mathbf{r}\})$, which is a superposition of all the pairwise potentials in the system. ∇_i is a short hand notation for gradients at position, $\mathbf{r}_i$, where the particle is located. Notice that the pair interaction potential depends only on the relative distance between particles.

The additional stochastic force is represented by an approximation of the random collisions between the particles. The stochastic force is assumed to be uncorrelated Gaussian white noise determined by its zero mean and variance, namely

$$
\begin{aligned}
\langle \mathbf{f}_i(t) \rangle &= 0 \\
\langle \mathbf{f}_i(t) \mathbf{f}_j(t') \rangle &= 2\gamma k_B T \delta_{ij} \delta_{t-t'},
\end{aligned}
\tag{3.3}
$$

where δ_{ij} is the unit $d \times d$ matrix, and $\delta_{t-t'}$ is the Kronecker symbol. These equations fulfill the dissipation-fluctuation relation, from which we have that the diffusion constant is related to mobility by $D = \gamma^{-1} k_B T$.

In the approximation that inertial effects are small, the evolution of a particle i at position $\mathbf{r}_i$ is derived by a Langevin equation on the form of Eq.(3.4). That is,

$$\gamma \frac{d\mathbf{r}_i}{dt} = -\nabla_i U(\{\mathbf{r}\}) + \mathbf{f}_i. \tag{3.4}$$

3.1.2   The Smoluchowski equation

A complete solution of a macroscopic system would contain the collection of all the solutions of the microscopic equations of the system. That is solutions of the Langevin equation for all the colloids in the system. Typically, the number of colloids in the system is large and hence it is costly to treat each particle independently. For a large collection of colloids it is more convenient to track the dynamics of the system collectively as in a continuous model. This approach is equivalent to investigate the stochastic processes by means of distribution functions, i.e. to track how the density distribution evolves in time. The collective behaviour can be interpreted in terms of the evolution of the configuration probability, $W(\{\mathbf{r}\}, t)$, of having N particles situated at positions $\{\mathbf{r}\} = \{\mathbf{r}_1 \cdots \mathbf{r}_N\}$ at an instant of time t. The collective dynamics in the system can be described by a set of coupled stochastic equations of motion, such as the Langevin equation, Eq.(3.4). Hence, the evolution of $W(\{\mathbf{r}\}, t)$ is determined from the set of N Langevin equations of the individual particles and satisfies the so-called Smoluchowski equation given as, [35],

$$\partial_t W(\{\mathbf{r}\}, t) = \frac{k_B T}{\gamma} \nabla^2 W + \frac{1}{2\gamma} \nabla \cdot \left(W \nabla \sum_{i \neq j} u(|\mathbf{r}_i - \mathbf{r}_j|) \right), \tag{3.5}$$

which determines the probability to find the set of N particles within a small value around the position $\{\mathbf{r}\}$ at time t, given a normalized initial distribution $W(\{\mathbf{r}\}, 0)$ [35].

From Eq. (3.5), we notice that in the absence of pair interactions, the second term on the rhs vanishes and as a consequence the system is described at a mesoscale by the classical diffusion equation. That is, Fick's law which predicts that the diffusion flux, responsible for the space and time evolution of the density distribution in a system, becomes proportional to $\nabla \rho$. For more complex, non-Fickian diffusion the additional deterministic interactions must be accounted for. Then the diffusive flux is controlled by gradients in the chemical potential, which here can be related by the second term on the rhs of Eq.(3.5).

As mentioned, Eq. (3.5) provides a description of the evolution of a N-point probability density,

$$\rho^{(N)}(\{\mathbf{r}\}, t) = W(\{\mathbf{r}\}, t), \tag{3.6}$$

with N-degrees of freedom. A more local description can be obtained by means of a 1-point density $\rho(\mathbf{r}, t)$ where the degrees of freedom are reduced by integration over all other variables $\{\mathbf{r}_2 \cdots \mathbf{r}_N\}$. The relation between a given n-th order probability density and the configuration density is given by

$$\rho^{(n)}(\{\mathbf{r}\}, t) \;\; = \;\; \frac{N!}{(N - n)!} \int \prod_{m=n+1}^{N} d^2 \mathbf{r}_m W(\{\mathbf{r}\}, t). \tag{3.7}$$

That is, the probability of a n-particle configuration is obtained by integrating up the $N - n$ degrees of freedom corresponding to the other particles that do not participate into this reduced configuration. All the particles are treated identically, which is accounted for by the combinatorial factor. Using the formula in Eq. (3.7), we have that the one point density and the two-point density are given as

$$
\begin{aligned}
\rho^{(1)}(\mathbf{r}, t) &= N \int \prod_{m=2}^{N} d^2\mathbf{r}_m W(\{\mathbf{r}\}, t) \\
\rho^{(2)}(\mathbf{r}, \mathbf{r}', t) &= N(N-1) \int \prod_{m=3}^{N} d^2\mathbf{r}_m W(\{\mathbf{r}\}, t).
\end{aligned}
\tag{3.8}
$$

Formally, the interaction potentials for the colloidal particles contain both short-range and long-range interactions and hence these potentials can be quite complicated. The nature of the interactions may however be simplified by assuming that the pair interactions dominate over the higher order interactions. Deviations from this identity arise in systems where the long-interaction forces cannot be neglected and the correlation between particles has to be treated. This is the case for instance in a crystal, where the long-range elastic forces between particles, impose a long-range crystal lattice order and hence strong correlation between particles in the lattice. Due to these long-range interactions, the diffusion process described by the Smoluchowski equation, Eq. (3.5), becomes very nontrivial.

An evolution equation for $\rho(\mathbf{r})$ can be obtained from Eq. (3.5), by applying a $N - 1$-dimensional integral over all the dummy degrees of freedom and arrive at

$$
\partial_t \rho(\mathbf{r}, t) = D\nabla^2 \rho(\mathbf{r}, t) + \gamma^{-1}\nabla \cdot \int d^2\mathbf{r}' \rho^{(2)}(|\mathbf{r} - \mathbf{r}'|, t)\nabla u(|\mathbf{r} - \mathbf{r}'|),
\tag{3.9}
$$

which is a continuity equation for the density. Notice that the equation reduces to Fick's diffusion equation for the system if the second term on the rhs vanishes. As previously discussed, that would correspond to a system in which there is no correlation between the colloidal particles. However, our system consists of interacting particles and is hence non-Fickian.

Now, recall that, to a large extend, the study of phase transitions involves the study of the dynamics of a system as it evolves towards a state in which the values of the physical parameters ensure equilibrium. A phase is stable in the parameter space which minimize the free energy functional, hence it is convenient to express the evolution of the density field as a function of a free energy functional. For our system the evolution of the density, Eq. (3.9), can be expressed as a generic non-Fickian diffusion along the gradient of a chemical potential $\mu = \delta\mathcal{F}/\delta\rho$, namely as

$$
\partial_t \rho = D\nabla \cdot \left(\rho(\mathbf{r})\nabla \frac{\delta\mathcal{F}\{\rho\}}{\delta\rho} \right).
\tag{3.10}
$$

That is, an expression for the density evolution in terms of the free energy functional $\mathcal{F}\{\rho\}$. Each of the terms of the rhs of Eq. (3.9) can be connected to the free energy by

identifying the individual terms as different energetic contributions. In the absence of contributions due to external fields, the total free energy is composed of two terms,

$$\mathcal{F}\{\rho\} = \mathcal{F}_{id}\{\rho\} + \mathcal{F}_{ex}\{\rho\}. \tag{3.11}$$

The first term in Eq. (3.11) represents the ideal gas free energy that corresponds to the Fickan diffusion term in Eq. (3.9). Thus, it represents the free energy of an ideal system consisting of non-interacting particles. It is determined by the entropic energy contributions and has the form

$$\mathcal{F}_{id}\{\rho\} = \int d^2\mathbf{r}\rho(\mathbf{r}) \left(\ln\left(\frac{\rho(\mathbf{r})}{\rho_0} \right) - 1 \right), \tag{3.12}$$

with derivative

$$\frac{\delta\mathcal{F}_{id}\{\rho\}}{\delta\rho} = \ln\left[\rho(\mathbf{r})\right], \tag{3.13}$$

apart from some additional constants that will disappear in the process of identifying the term on the form in Eq.(3.10) and hence is of less importance.

For a system consisting of interacting particles, there is an additional contribution to the free energy functional which is interpreted by the second energy term in Eq. (3.11). This excess energy represents the non-ideal interactions between particles and is more difficult than the ideal term. The first order density function is now dependent on second order correlations, which have to be provided a priori. The excess free energy is related to the second term in Eq. (3.9) by the identity, [35],

$$\nabla\frac{\delta\mathcal{F}_{ex}\{\rho\}}{\delta\rho} = \frac{1}{D\gamma} \int d^2\mathbf{r}'\frac{\rho^{(2)}(|\mathbf{r} - \mathbf{r}'|, t)}{\rho(\mathbf{r}, t)}\nabla u(|\mathbf{r} - \mathbf{r}'|), \tag{3.14}$$

but is yet to be specified.

In the next section, we provide a set of simplifications that allows us to reduce the expressions for the free energy such that they only depend on the local density $\rho(\mathbf{r})$ and its gradients. Hence, we will arrive at the phase field crystal model, equivalent to the phenomenological model proposed by Elder et al. in [12].

3.1.3 The Phase field crystal equation

A suitable expression for the free energy functional is yet to be specified. As previously mentioned, we want the free energy functional to minimize to a periodic density field and thereby include the elastic energy and symmetry properties of a crystalline material. Hence, it is convenient to have a free energy functional which is only dependent on the local density. Equivalent to the phase field method, the density field, $\rho(\mathbf{r})$, in the phase field crystal method is regarded as a phase field, $\psi(\mathbf{r})$. Hence, the

density dependent free energy functional is interpreted as a function of the phase field, that is $\mathcal{F}\{\rho(\mathbf{r})\} = \mathcal{F}\{\psi(\mathbf{r})\}$. To obtain the expression for the free energy functional in terms of the phase field parameter, three main simplifications are carried through.

First, we assume that the mobility, ρD, in the diffusion equation, Eq.(3.10), is constant. By this assumption, we claim that the contribution from a heterogeneous mobility coefficient from the density variations is negligible. The density, $\rho(\mathbf{r})$, in front of the functional derivative is represented by a constant equilibrium mean density, that is $\rho(\mathbf{r}) = \rho_0$. We can thereby approximate an effective diffusion constant $\bar{D} = D\rho_0$ and express Eq. (3.10) as

$$\partial_t \rho = \bar{D}\nabla^2 \frac{\delta \mathcal{F}\{\rho\}}{\delta \rho}. \tag{3.15}$$

The second approximation is an approximation of the ideal free energy in Eq. (3.12). A suitable expression for the logarithmic ideal free energy is obtained through a Taylor expansion of the logarithm relative to the equilibrium reference density ρ_0. We define the relative units $\psi(\mathbf{r}) = (\rho(\mathbf{r}) - \rho_0)/\rho_0$, a dimensionless phase field parameter which describes the density field relative to the previously defined equilibrium density, ρ_0. The coefficients in front of the Taylor expansion are chosen so that we arrive at the double-well potential with a tunable well-depth in terms of the α parameter. Disregarding the constant terms, we have that the ideal free energy part reduces to

$$\mathcal{F}_{id}\{\psi(\mathbf{r},t)\} = \int d^2\mathbf{r} \left(\frac{\alpha}{2}\psi^2 + \frac{1}{4}\psi^4 \right). \tag{3.16}$$

We have now obtained an expression for the ideal free energy in terms of the relative $\psi(\mathbf{r},t)$ units. Keep in mind that the temperature parameter must be negative, i.e. $\alpha = (T - T_c)/T_c < 0$, in order to obtain the double well potential.

The non-ideal free energy contribution, represented by the excess free energy, is the term which generates the periodic structure in the material. Thus, it is an important part of the phase field crystal model and a density dependent expression for the excess free energy in terms of the order parameter is obtained through a last approximation. A gradient expansion of the excess energy defined by Eq. (3.14), is performed also in the relative $\psi(\mathbf{r},t)$ units. Truncating the expansion on the fourth order and rearranging the corresponding terms, it can be shown that the excess energy reduces to the following functional form [35],

$$\mathcal{F}_{ex}\{\psi(\mathbf{r},t)\} = \kappa \int d^2\mathbf{r} \frac{\psi}{2} \left(1 + \nabla^2 \right)^2 \psi, \tag{3.17}$$

where $\kappa = 1/\gamma D$.

Under these approximations, we have obtained an expression for the free energy functional which minimizes to a periodic density field. The expression is given by means of a phase field parameter, $\psi(\mathbf{r})$, which describes the density field relative to the mean equilibrium density, ρ_0. The evolution of the relative density field can be

described by the following equation

$$\partial_t\psi(\mathbf{r}) = D\nabla^2\left(\alpha\psi + \psi^3 + (1+\nabla^2)^2\psi\right),\tag{3.18}$$

which is recognized as the phase field crystal equation proposed in a phenomeno-
logical model by Elder et al. in [12]. Notice that the equation of motion is constrained
by conservation of the density field.

As previously discussed, a state of matter is determined by the value of the state
variables, here represented by density and temperature, that is $\rho(\mathbf{r})$ and α. In a
two dimensional system, there are three equilibrium phases representing the three
distinct solutions for $\psi(\mathbf{r})$. That is, the free energy functional is minimized by different
solutions resulting in phases with different periodic patterns; the constant phase,
the stripe phase or the triangular phase, the latter being the crystalline phase. In
Fig.(3.1) we present a two dimensional phase diagram calculated in the one mode
approximation by Elder et al. in Ref. [11].
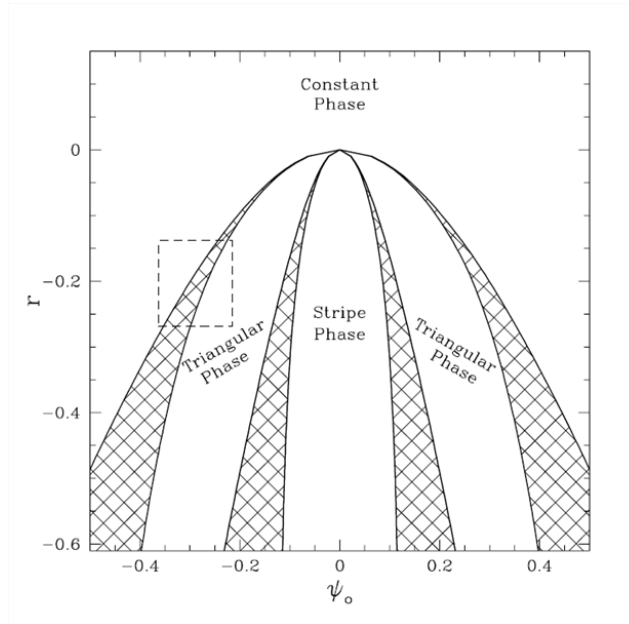
Figure 3.1: Two dimensional phase diagram calculated in the one mode approximation
by Elder et. al. The constant phase, the stripe phase and the triangular phase
represent the equilibrium states for the three disinct solutions for $\psi(\mathbf{r})$, while the
hatched areas correspond to regions of coexistance. The different phases can be
obtained by varying the values of the state variables, r and $\psi(\mathbf{r})$, where the former
corresponds to the tunable temperature parameter, i.e. $r = \alpha$

By varying the values of α and $\psi_0(mathbfr)$ we can obtain equilibrium states
with different patterns. In addition, we can obtain systems in which different states
of matter coexist, in Fig.(3.1) this situation is presented as hatched areas.

3.2 The dynamics of a phase transition

In the previous chapter, we discussed the process of phase transitions for both conserved and non-conserved density fields through phase field modeling. We considered disordered binary systems in which the species was characterized by different densities. The initial homogeneous system was driven out of its prefered equilibrium by a rapid drop in temperature and the evolution of the density field towards a new equilibrium was investigated. Recall that the free energy functional then was minimized by uniform density fields and that for a conserved density field we arrived at the Cahn-Hilliard equation,

$$\partial_t \psi(\mathbf{r}) = D\nabla^2 \left(\alpha\psi + \psi^3 - \nabla^2\psi \right), \tag{3.19}$$

as an equation for describing the dynamics of the relaxation process, where D now denotes the constant mobility.

Recall that the ideal contribution to the free energy in the PFC-model was constructed as a symmetrical double-well potential with a tunable well-depth in terms of the α -parameter, that is by the Landau free energy. In the previous chapter, we derived the CH- equation and the Ginzberg-Landau equation with the same free energy funtional. Then, the ideal contribution was modified by a non-local term to account for the energy cost of having heterogeneities near the interface. In the PFC-equation, the modification is extended and renders a spatial structure of the density field in equilibrium. The spatial structure is provided through the excess free energy by including the contributions from long-range interactions in the interaction potential. Hence, the PFC-equation, Eq.(3.18), describes the evolution of a time-averaged density field, subjected to the constraint of density conservation [1] and provides thereby an extension of the Cahn-Hilliard equation, in which the density field is averaged in both time and space.

In the following paragraph, we investigate a phase transition in a two dimensional system in which the dynamics of the conserved density field is governed by the PFC-equation. We consider the same simple physical system as in the previous chapter, that is a homogeneous mixture of two species characterized by different densities. A sudden drop in temperature drives the system out of its equilibrium state and the evolution towards a new equilibrium state starts. Fig.(3.2), depicts snapshots of the evolution of the density field as it reorganizes on the path towards the new equilibrium state. In this simulation, the parameter values,α and ψ_0 are chosen from Fig.(3.1) to ensure a periodic crystalline structure in equilibrium.
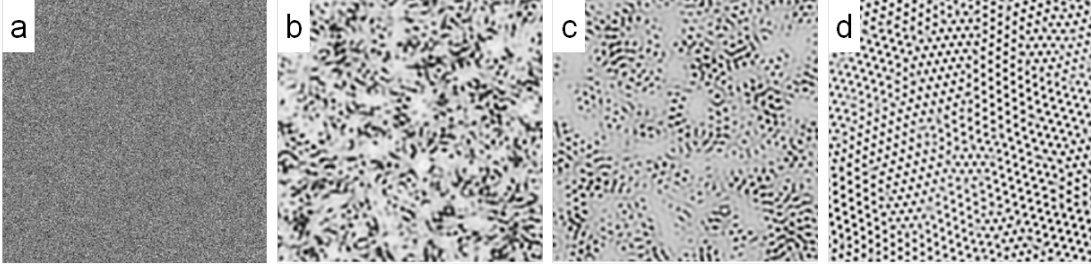
Figure 3.2: Snapshots of the temporal evolution of a quenched system. (a),(b),(c) and (d) represent the initial homogeneous system and three successive later times. The initial disordered species reorganize into a periodic structure. The numerical simulation is performed with undercooling parameter and mean density, $\alpha = r = -0.25$ and $\psi_0 = 0.25$. That is, values which in the parameter space correspond to the regime where the the system relaxes to a crystalline structure. System size $nx = ny = 500$.

The dynamics of the phase transition in Fig.(3.2) was governed by the PFC-equation and the figure depicts the time evolution as the two species reorganize into a periodic structure. The pattern of the density field in the new equilibrium state is dependent on the value of the equilibrium mean density, ρ_0, and the temperature in the system. The latter is here represented by means of the dimensionless undercooling parameter, $\alpha = (T - T_c)/T_c$.

So far, we have discussed phase transitions and how its nature is dependent on the equations governing the phase dynamics in the system as well as on the values of the state variables. The former is determined by the choice of free energy functional and the constraints on the dynamics in the system, while the later is chosen from the phase diagram depicted in Fig.(3.1). In Fig.(3.3) we illustrate the differences by a comparison of patterns generated in phase transitions governed by different differential equations. Late stage pictures from the evolution process for both non-conserved and conserved parameter fields with both uniform and periodic density fields are depicted in the figure. The phase dynamics in the four systems,(a)-(d), are governed by the Ginzberg-Landau -, the Swift-Hohenberg, the Cahn-Hilliard- and the phase field crystal - equations respectively. From the point of view of pattern formation theory, the PFC equation is a conserved analogue of the Swift-Hohenberg equation [1]. The SH-equation reads as,

$$\partial_t \psi(\mathbf{r}) = D \left(-\alpha\psi - \psi^3 - (1 + \nabla^2)^2\psi \right), \tag{3.20}$$

whilst the Ginzberg-Landau and Cahn-Hilliard -equations are the phase field equations we discussed in the previous chapter.
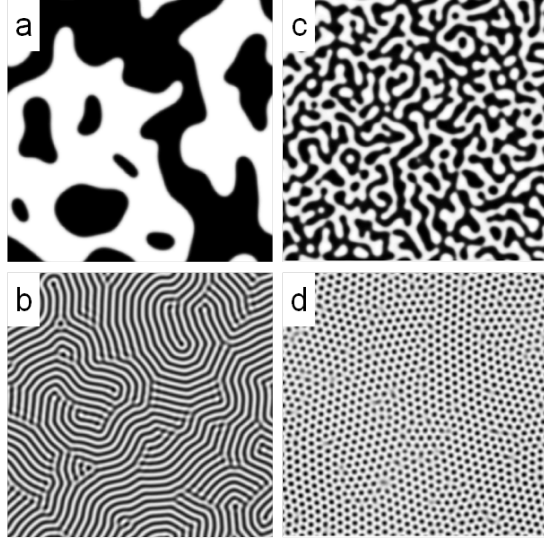
Figure 3.3: Pictures (a),(b),(c) and (d) represent pattern formation due to disorder-order processes in binary systems, all at a late times, and illustrates the dependence of the governing differential equations. The patterns originates from the same initial heterogeneous system consisting of two species characterized by their different densities. The dynamics of the phase transitions are governed by the Ginzberg-Landau, Swift-Hohenberg, Cahn-Hilliard and PFC-equations respectively. The numerical simulations are performed in a system with state variables $\alpha = -0.25$ and $\psi_0 = 0.25$ for PFC and SH, and $\alpha = -1$ and $\psi_0 = 0$ for GL and CH. System sizes $nx = ny = 500$.

Fig.(3.3) illustrates the difference between the phase field method and the phase field crystal method. In the PF-method, the density field is averaged in both space and time, and hence posess uniform density fields, as illustrated in pictures (a) and (c). In contrast, the PFC-method (as well as the SH equation) averages in time, but leaves a spatially variating density field, as depicted in Fig.(3.3(d)). The additional constraints on the free energy functional ensure periodic equilibrium states and hence give the possibility of simulating microsctructural evolution at diffusive time scales. This is a fundamental feature of the phase field crystal model.

According to Ref. [11], the basic physical features of elasticity is naturally incorporated by any free energy that is minimized by a spatially periodic function. Hence, by constructing phase fields which prefer to be periodic in space, the phase field crystal method possess a useful method to describe various properties of crystalline materials. In Ref. [11], Elder et al. argue that the method is capable of capturing features such as the energy of grain boundaries separating two phases, epitaxial growth and yield strength of crystalline materials.

The dissipative dynamics in the phase transition is driven by free energy minimization and the form of the free energy functional determines the symmetry of the crystalline structure. According to Ref. [11], there is no systematical way of deter-

mining the crystal symmetry by adjusting the free energy functional, but it is known that it is determined by the choice of non-linear terms in the free energy functional. The free energy functional that we present here is of a simple form and will always produce a triangular lattice in two dimensions. In three dimensions, the same choice of free energy functional will give the body centered cubic structure.

The structure of the density field repeats itself consistently in time and space, similar to the shape of a wave. In a single mode approximation, the density field can be decomposed into periodic density waves with characteristic amplitudes. Hence, we can investigate liquid-solid phase transitions through the dynamics of the amplitudes in the solid phase.

3.3   The Amplitude equations

In this section, we discuss the density waves in the crystalline phase, represented by their amplitudes. Let us recall the phase field crystal equation that was previously derived. In a non-dimensional form, it is given by

$$\partial_t \psi = \nabla^2 \left(\alpha\psi + \psi^3 + (1 + \nabla^2)^2 \psi \right), \tag{3.21}$$

where $\alpha = (T - T_c)/T_c$ is the undercooling parameter relative to the critical temperature. In the liquid phase, the density field is uniform and will take a homogeneous value, say ψ_l. In the solid phase, the spatially variating density field, $\psi_s(\mathbf{x}, t)$, can be decomposed into a homogeneous mean density $\bar{\psi}$ and heterogeneously superimposed density fluctuations, $\tilde{\psi}(\mathbf{x}, t)$. That is, $\psi_s = \bar{\psi} + \tilde{\psi}$. By inserting this decomposition into Eq. (3.18), we obtain that the density fluctuations satisfy in the limit of small variations, i.e. $|\tilde{\psi}| \ll 1$, a linearized equation on the form

$$\partial_t \tilde{\psi} = \nabla^2 \left(\alpha\tilde{\psi} + 3\bar{\psi}^2\tilde{\psi} + (1 + \nabla^2)^2\tilde{\psi} \right). \tag{3.22}$$

For a perfect crystal phase, the density fluctuations have a periodic structure with the crystal-lattice symmetry, which in two dimensions is triangular. Hence, the free energy functional is minimized by three distinct solutions for $\psi_s(\mathbf{r}, t)$ and we can decompose $\tilde{\psi}(\mathbf{x}, t)$ into a superposition of three planar waves. The waves are characterized by the same constant amplitude, $A(t)$, and the corresponding reciprocal wave-vectors, $\mathbf{k}_j$ with $j = 1, 2, 3$. Thus,

$$\tilde{\psi}(\mathbf{x}, t) = A(t) \sum_{j=1}^{3} \left(e^{i\mathbf{k}_j \cdot \mathbf{x}} + e^{-i\mathbf{k}_j \cdot \mathbf{x}} \right), \tag{3.23}$$

where the lattice vectors representing a hexagonal crystal are given by

$$\mathbf{k}_1 = -\frac{\sqrt{3}}{2}\mathbf{i} - \frac{1}{2}\mathbf{j}, \quad \mathbf{k}_2 = \mathbf{j}, \quad \mathbf{k}_3 = \frac{\sqrt{3}}{2}\mathbf{i} - \frac{1}{2}\mathbf{j}, \tag{3.24}$$

with $\mathbf{i}$ and $\mathbf{j}$ being the unit vectors in the xy-plane. In order to obtain translational invariance between the crystal-lattice and the reciprocal lattice, the k-vectors must satisfy the following properties: $|\mathbf{k}_j| = 1$ for every $j = 1, 2, 3$ and $\sum_{j=1}^{3} \mathbf{k}_j = 0$.

By combining the form of density fluctuations in a perfect crystal from Eq. (3.23) with the evolution of these small perturbations as in Eq. (3.22), we find that the uniform crystal amplitude, $A(t)$, satifies the following equation

$$\partial_t A(t) = -|\mathbf{k}_j|^2 \left(\alpha + 3\bar{\psi}^2 + (1 - |\mathbf{k}_j|^2)^2 \right) A(t). \tag{3.25}$$

Since the prefactor on the rhs is constant and, in fact, simply left to being $-(\alpha + 3\bar{\psi}^2)$ for unit k-vectors (see the property above), it follows that the above equation has an exponential solution as $A(t) = A_0 e^{\omega t}$, determined by a constant growth rate equal to $\omega = -\alpha - 3\bar{\psi}^2$. Hence, for $\omega < 0$, the crystal amplitude decays exponentially to zero, and with it, so the density fluctuations vanish leaving behind a stable uniform density. In this way, we can determine the values of the state parameters which gives the constant equilibrium phase depicted in Fig.(3.1). That is,

$$\begin{aligned} \omega = -\alpha - 3\bar{\psi}_0^2 &< 0 \\ \sqrt{-\alpha/3} &< |\bar{\psi}_0|. \end{aligned} \tag{3.26}$$

Hence, the uniform liquid phase is dynamically stable for the state variables which satisfy the stability requirement , $\sqrt{-\alpha/3} < |\bar{\psi}_0|$. In the next section we will examine the process of a single crystal growing from an undercooled liquid by means of the periodic density fields, as well as through the dynamics of the amplitude fields.

3.3.1 Growth of single crystals

Recall from the previous chapter, the investigation of the growth mechanics of a droplet in a binary system through the phase field model. A single droplet, referring to a solid phase, surrounded by a liquid phase started to grow when the temperature in the system was quenched. As previously discussed, the phase field method is restricted to the case of isotropic growth. In this section, we will examine the growing crystal through the PFC-model and hence provide a periodic structure in the solid phase which is capable of capturing anisotropy. The initial system is now constructed as a droplet with periodic density field surrounded by a homogeneous liquid phase. In Fig.(3.4) we present the evolution of a single crystal growing from the surrounding undercooled liquid.
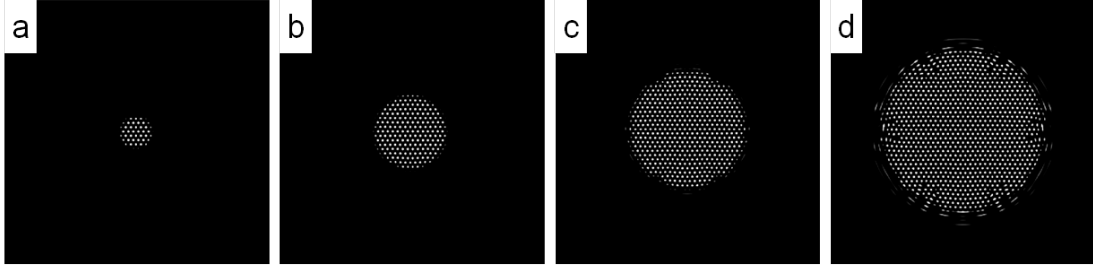
Figure 3.4: Pictures (a)-(d) illustrates growth in a two dimensional system at successive time steps. The droplet grows radially outwards after a rapid temperature drop. The liquid phase is represented by a uniform density field, while the growing crystal is represented by a periodic density structure. The roughening of the crystal surface in the later stage suggests surface instabilities in the system which leads to dendritic patterns. Undercooling parameter and mean density $\alpha = -0.25$ and $\psi = 0.25$. These parameter values are chosen from the phase diagram to ensure a dynamically stable crystalline phase. System size $nx = ny = 500$.

We have now investigated the growth of a blob through both the phase field method and the phase field crystal method. A comparison of the single crystal in the phase transition for the two method is presented in Fig.(3.5). In the PF-method, both the crystal and the liquid phase possess a uniform density field, while a feature of the phase field crystal method is its ability to capture the spatial structure of the solid phase.
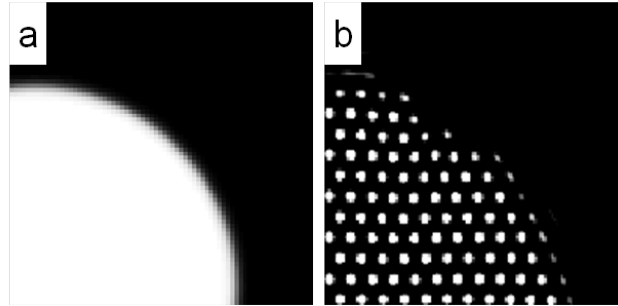
Figure 3.5: Pictures (a) and (b) represent the density fields of a single crystal surrounded by a liquid phase constructed by the PF-method and the PFC-method, respectively. The PF-method simulates both the crystal phase and the liquid phase by homogeneous density fields, separated by a diffuse interface. The PFC-method captures the periodic structure of the crystal phase, whilst the liquid phase is represented by a homogeneous density field. The two phases are separated by a diffuse interface. Undercooling parameter and mean densities are $\alpha = -0.25$ and $\psi = 0.25$. System sizes $nx = ny = 500$.

The evolution of the crystalline material can also be examined by means of the amplitude equations, Eq.(3.25). In Fig.(3.6) we present the density field and the amplitude field of a single crystal in a liquid phase, simulated by the PFC-method.
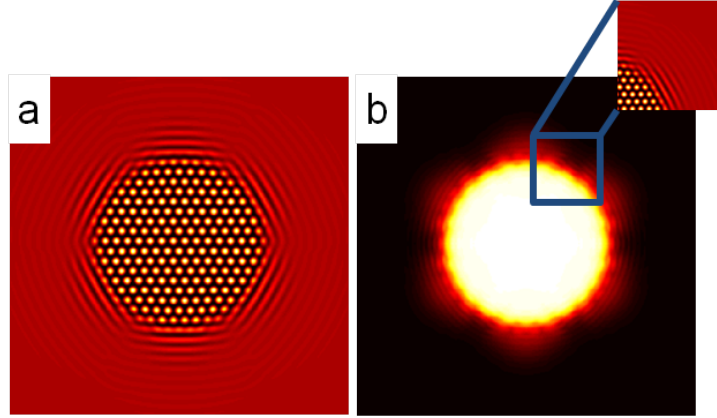

Figure 3.6: (a) represents the density field of a single crystal surrounded by a liquid phase. The density field has a periodic structure within the crystalline phase, while the liquid phase is represented by a homogeneous density field. (b) represents the amplitude field of the same single crystal and its surrounding liquid. Notice that the amplitude field is constant inside the crystal, vanishes in the liquid phase whilst it changes rapidly across the solid-liquid interface. The density field connected to (b) is a cut out of the density field depicted in (a). Undercooling parameter and mean density for the system is $\alpha = -0.6$ and $\alpha = 0.39$ respectively. System Size $nx = ny = 1024$.

So far, we have discussed the case of single crystals. But the conditions under which a single crystal can grow progressively without disturbance are straight. That is, from the very beginning of the solidification process, there can only be a single crystal surrounded by a liquid phase. In nature, it is however more likely that the solidification starts from a system consisting of several seeds growing simultaneously with atomic structures in accordance with the structure of each seed. There is however no reason for all the crystals to have the same lattice orientation. That is, the solidification process is likely to form what we call a polycrystalline material consisting of single crystals with different lattice orientations which have grown together.

What happens though, with the dynamics of the density field, when there are many crystals having different orientations? In the next section we will generalize the density fluctuations for a single crystal in Eq. (3.23) to represent a polycrystalline material.

3.3.2   From single crystals to polycrystalline materials

In general, a solidified mass consists of a collection of single crystal grains grown together and separated by grain boundaries. The individual grains are periodic in structure, but the different lattice orientations breaks the periodicity across the grain boundaries. The broken periodicity breaks the crystal rotational symmetry and hence, the grain boundaries can be seen as defects in the system. The PFC-method can incorporate such defects and is thereby suitable to describe the evolution of several crystals of arbitrary orientation that collides and form grain boundaries [1]. By relaxing the assumption of a constant amplitude for the density fluctuations for a single crystal, Eq. (3.23) can be generalized to represent a polycrystalline material.

We assign a spacially-dependent amplitude $A_j(\mathbf{x}, t)$ for each mode $j = 1, 2, 3$ and derive amplitude equations governing the dynamics of each of these modes. On the whole, these amplitudes are constant inside each crystal, vanish in the liquid phase and have sharp gradients across grain boundaries. Since all the crystals are expanded relative to a base crystal orientation with the wave-vectors $\mathbf{k}_j$, the relative misorientation between grains is consequently incorporated in the complex phase of the amplitudes. Hence, for a polycrystalline phase we consider a generic amplitude expansion of the density fluctuations on the form

$$\tilde{\psi}(\mathbf{x}, t) = \sum_{j=1}^{3} \left(A_j(\mathbf{x}, t) e^{i\mathbf{k}_j \cdot \mathbf{x}} + A_j^*(\mathbf{x}, t) e^{-i\mathbf{k}_j \cdot \mathbf{x}} \right), \tag{3.27}$$

where the complex conjugate of the amplitude is denoted by the upper star index, i.e. A^*. The evolution of these complex amplitudes follows from the governing equation of the density field, that is the phase field equation, given in Eq. (3.18). The PFC-equation is however strongly non-linear and we will in the following treat the linear terms seperately from the more difficult non-linear coupling terms between the amplitudes and their complex conjugates.

The linear part can be straighforwardly obtained by inserting Eq. (3.27) into the linearized equation

$$\partial_t \tilde{\psi} = \nabla^2 \left(\alpha \tilde{\psi} + 3\overline{\psi}^2 \tilde{\psi} + (1 + \nabla^2)^2 \tilde{\psi} \right), \tag{3.28}$$

representing the dynamics of the density fluctuations in the limit of small variations, i.e. $|\tilde{\psi}| \ll 1$, equivalent to Eq.(3.22). In the linear regime, the modes decouple and we can treat them seperately. Each of the modes satisfy the following equation

$$\partial_t A_j(\mathbf{x}, t) = (1 - \mathcal{L}_j) \left(-\alpha - 3\overline{\psi}^2 - \mathcal{L}_j^2 \right) A_j(\mathbf{x}, t), \tag{3.29}$$

where $\mathcal{L}_j = (\nabla^2 + 2i\mathbf{k}_j \cdot \nabla)$ denotes the differential operator corresponding to $(\nabla^2 + 1)$ when it acts upon $A_j(\mathbf{x}, t) e^{i\mathbf{k} \cdot \mathbf{x}}$ for each of the modes, $j = 1, 2, 3$.

The additional nonlinear coupling terms come from expanding the cubic nonlinear part in Eq. (3.18), that is

$$(\overline{\psi} + \tilde{\psi})^3 = \overline{\psi}^3 + 3\overline{\psi}^2 \tilde{\psi} + 3\overline{\psi} \tilde{\psi}^2 + \tilde{\psi}^3, \tag{3.30}$$

where $\tilde{\psi}(\mathbf{x}, t)$ is given by Eq. (3.27). The first term in the equation above disappears from the equation of motion when the mean density is homogeneous. The second term represents the linear part that we have just taken into account, whilst the last two terms yield the nonlinear amplitude couplings. The last step in the derivation of the equations of motion for the amplitude field of a polycrystalline material is to obtain expressions for these non-linear coupling terms. We can obtain this by inserting the amplitude expansion of the density fluctuations into the last two terms and using the properties of the k-vectors.

Then we arrive at the following nonlinear equation for the $j = 1$ -mode amplitude, A_1,

$$\partial_t A_1 = (1 - \mathcal{L}_1)\left(-\alpha - 3\bar{\psi}^2 - \mathcal{L}_1^2 - 3(|A_1|^2 + 2|A_2|^2 + 2|A_3|^2)\right) A_1. \quad (3.31)$$

Similar equations describe the evolution of A_2 and A_3 by the corresponding index permutation.

Similar to the case of the single crystal, we can now examine polycrystalline material by means of both periodic density fields and the amplitude fields. In Fig.(3.7) we present the density field, $\psi(\mathbf{r}, t)$, and the amplitude field of a polycrystalline material, simulated by the PFC-method.
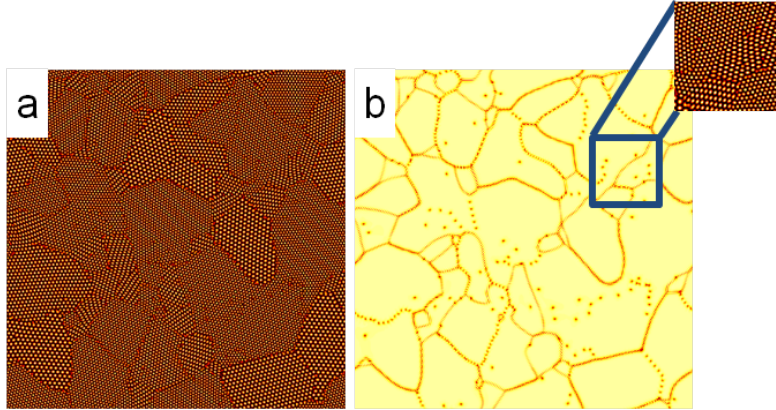
Figure 3.7: (a) Represents the density field of a polycrystalline material. The density field is a result of several individual crystals of same hexagonal periodicity but arbitrary lattice orientation which have grown together. As the individual crystals collide, they form grain boundaries which separate grains of different orientations. Notice that the pattern is periodic inside each grain and that there is a break in the periodicity across the grain boundaries. (b) depicts the amplitude field of the same polycrystalline material as depicted in (a). Notice that the amplitude field is homogeneous inside each grain and vary rapidly across the grain boundaries and across other defects in the material. The latter is recognized as 'red dots' in the amplitude field. The density field connected to (b) is an out cut of the density field depicted in (a). Undercooling parameter and mean density for the system is $\alpha = -0.6$ and $\alpha = 0.39$ respectively. System Size $nx = ny = 1024$.

We have now derived equations of motion for the amplitudes of periodic density fields and examined the density fields and amplitude fields for both single crystals and polycrystalline materials. The values of the state variables was chosen from the phase diagram in Fig.(3.1), to ensure that the system relaxed into the crystalline phase. Recall that, in the previous derivations, we decomposed the density field into a constant mean density and periodically variating density fluctuations, i.e. $\psi(\mathbf{r}, t) = \bar{\psi}(\mathbf{r}, t) + \tilde{\psi}(\mathbf{r}, t)$. The approximation of having a homogeneous mean density in space is valid for single-phase systems, but fails to describe regions of coexistance, represented as hatched areas in the phase diagram. In these regions we have a two-phase system in which liquid is at coexistance with the crystal phase. Hence, there can be density variations across the liquid-solid interface and the approximation of having a homogeneous mean density in space is not longer valid.

In Ref. [38], Yeon et al. present an extended amplitude formulation for the density waves that does not restrict the amplitude equations to single-phase systems. The space dependence of the mean density, i.e. $\bar{\psi}(\mathbf{x}, t)$, is taken into account by use of a multiple scale analysis. The basic of this method is to take advantage of the fact that the average density and amplitudes vary at larger length and time scales than the density fluctuations [38]. Hence, a small parameter, ϵ, can be introduced to scale the

arguments for the amplitude equations and the density field. The now slowly varying mean density field, $\bar{\psi}(\mathbf{x}, t)$, is thereafter expanded in powers of ϵ. The equations of motion for the mean density field and the amplitudes are obtained by substituting the extended and scaled expansion of $\psi(\mathbf{x}, t)$ in the PFC-equation. By rescaling the new evolution equations back to the original variables, the additional equations of motion governing the mean density field is obtained,

$$\partial_t \bar{\psi} = \nabla^2 \left(\alpha \bar{\psi} + 3\bar{\psi}\tilde{\psi}^2 + (1 + \nabla^2)^2 \bar{\psi} + \bar{\psi}^3 + 6 \left(\prod_{i=1}^{3} A_i + \prod_{i=1}^{3} A_i^* \right) \right). \tag{3.32}$$

By substituting $\sum_{i=1}^{3} |A_i|^2 = \tilde{\psi}^2$ for the second term on the rhs, the three first terms on the rhs corresponds to the linear terms, equivalent to the linearized equation of motion for the density fluctuations given in Eq.(3.28).

The dynamics of the amplitudes are given as

$$\partial_t A_1 = (1 - \mathcal{L}) \left(-\alpha - 3\bar{\psi}^2 - \mathcal{L}_1^2 - 3(|A_1|^2 + 2|A_2|^2 + 2|A_3|^2) \right) A_1, \tag{3.33}$$

equivalent to Eq.(3.31). In this model for a two-phase system, the approximation of a constant mean density is relaxed and the system is described by equations of motion for the amplitude field and the mean density, in Eq.(3.33) and Eq.(3.32), respectively.

We have now derived the phase field crystal model, a method which represents the crystalline phase by a periodic density field and hence incorporates physical features, such as impurities and grain boundaries. In the one mode approximation, the periodic structure of a crystalline materials can be decomposed into periodic density waves with characteristic amplitudes. We have presented equations of motion for these amplitudes which gives the possibility of invetigation the evolution of a phase transition by means of the dynamics of the amplitude fields. This method provides a suitable for investigating changes of state. In the next chapter, we will present our results from the investigation of phase transitions between liquid and crystalline materials, i.e. melting and freezing, through the PFC-method.

Chapter 4

Liquid-solid phase transitions

In the previous chapters we argued that the PFC-method provides a good description for the liquid-solid phase transition and studied simple physical systems in order to investigate the dynamics of such phase transitions. Additionaly, we derived amplitude equations capable of describing the crystalline phases on larger lengthscale. As a phase transition, melting of crystals is a common phenomena in nature. Dislocation mediated melting is a common theoretical approach to describe two dimensional melting with two plausible scenarios, that is the KTHNY-melting process and the grain boundary induced melting. The small scale details for crystal breakdown bring up challenges, however. In this chapter will will discuss the nature of melting and freezing on thin films that can be approximated as two dimensional systems. We focus on the small-scale mechanisms of melting crystals and discuss the role of defects through the phase transition.

In the study of phase transitions, progress has been made within both experimental work, theoretical theories as well as within numerical simulations. We will here present our numerical investigaton of freezing and melting and evaluate our results upon the two most relevant theories within dislocation mediated melting, i.e. the KTHNY- and grain-boundary-scenarios.

4.1   A change of state

Matter in different states and the process of transformation between the phases of matter has fascinated humans and challenged scientists for centuries. Of all the phenomena exhibited by condensed matter, changes of state are of the most dramatic and have stimulated development of quantum mechanics and classical thermodynamics. Various concepts, such as the role of dimensionality and the impact of impurities, such as dislocations, have been incorporated in the search of a full understanding of the small-scale details for the melting mechanism, [8, 32].

The different states of condensed matter can be classified by the range of order in the system. While a perfect crystalline solid is recognized by its order and periodic

lattice structure, a liquid phase is homogeneous with randomly distributed atoms and appears as a disordered system. Hence, the melting transition can be interpreted as a breakdown of the periodic order in a system with crystal symmetry. Investigating the nature of this reduction process can hence be a method to characterize the melting mechanism and to reveal its universalities.

Real systems usually consist of large amount of particles, which for convenience are treated on a coarse grained level by means of statistical mechanics. Hence, the density provides a coarse grained description of matter. In the previous chapters we treated phase transitions through the energy functionals Ginzberg-Landau and Cahn-Hilliard, represented in terms of the dimensionless order parameter, related to the density by $\psi(\mathbf{r}, t) = (\rho - \rho_0)/\rho_0$.

By creating simple models which captures the essential physics of the system, we can extract a clear understanding of the physics leading to a specific behavior [37]. Through models which can incorporate defects, we can investigate the cooperative interactions between dislocations in a crystalline material. The nature of the dislocation interactions is one of the aspects that separate the various theories of melting. Both the dislocation unbinding theory, by Kosterlitz, Thouless, Halperin, Nelson and Young, and the grain-boundary theory, by Chui, are based the dislocation energy, in analogy to the well-known treatment of a magnetic system in terms of a spin Hamiltonian [32].

The transformation between the solid and liquid state is a common phase transition in nature. As previously discussed, the state of matter is determined by the energy in the system, that is the energy which we perceive as temperature. For low temperatures, the system takes the ordered solid state, whilst the disordered liquid state is formed when the temperature is high enough to break the rigid structure of the solid. In the PFC-model, the solid state is represented by a density field which is periodic in space, while the liquid state has a homogeneous density field represented by the equilibrium mean density, $\rho_0(\mathbf{r}) = \rho$.

Though one could expect freezing and melting to be opposite of each other, these phase transitions are actually described by different small scale mechanics. Some work has been done in generalizing the two processes, and there has been great progress in understanding each of them, but a general theory of freezing and melting is still to be constructed [20].

Freezing is treated within a liquid-based theory, in which the process is described as condensation of the liquid phase. The process of crystallization is a spontaneous appearance of periodic order in a disordered system, [20], and the solidification process is associated with release of latent heat. On the other hand, the melting process is often discussed within a crystal-based theory where the ordered crystal lattice breaks down and leaves a uniform liquid. The melting transition occurs in systems of interacting particles, that is, systems in which the particles behave collectively and hence require a rigorous treatment. Most crystalline materials carry imperfections, i.e. contain defects such as dislocations, in the crystalline structure. The presence of

dislocations in the system affect the energy functional and is hence expected to have an impact on the melting temperature. Dislocation mediated melting is a common theoretical approach to describe the melting transition and we will in the following sections discuss some of the aspects that contribute to the nature of the melting transition, in particular, but as a counterpart, the process of freezing will also be discussed.

4.1.1 Continuous vs first order transition

One of the biggest puzzels in understanding the melting scenario is to determine the order of the phase transition which can occur in the thermodynamical limit [9]. As previously discussed, the different phases can be characterized by certain macroscopic properties, such as density. For convenience, these properties can be represented by a dimensionless order parameter, $\psi(\mathbf{r}, t) = (\rho - \rho_0)/\rho_0$, which gives the density in a certain area of the system relative to the equilibrium mean density of the system. During a phase transition, the system reorganizes and hence the value of $\psi(\mathbf{r}, t)$ changes. As the order parameter represents the density of the matter, its behaviour through a transition can indicate the order of the transition. Whilst a first order transition is abrupt and causes a discontinuously jump in the order parameter, a continuous transition is less sudden and the order parameter will change gradually [23].

Through a continuous phase transition, the properties of the matter change gradually and the transition can be described as a transition within one phase rather than a transition between two phases. According to Landau's theory, a continuous phase transition can only occur if certain symmetry conditions are satisfied [23]. That is, there can be no cubic term in the free energy functional, thus we obtain a symmetrical double well potential. An additional feature of this gradual change of state is the lack of latent heat connected to the phase transition.

A first order transition is abrupt, i.e. the material properties changes discontinuously. As opposed to a continuous transition, there are no symmetry requirements in the system. That means that there are no restrictions on the order of the functional which describes the energy in the system. The double well potential might very well be non-symmetrical and hence, the appearance of a cubic term in the energy functional will in general cause a first order transition to occur. Additionally, the transition is dismissive and requires a finite latent heat.

The order of a phase transition determines its dynamically nature as well as the evolution of the state variables. Hence, revealing the order of the melting transition is of importance for understanding the melting mechanism. In the following sections we will investigate the phase transition between liquids and solids, that is freezing and melting, in two dimensions using the phase field crystal model presented in the previous chapter.

4.2   Freezing

As previously mentioned, freezing is recognized as a spontaneous appearance of order in a disordered system. The phase transition is of first order, [20], and can occur if a uniform liquid state is turned dynamically unstable, e.g. through rapid changes in the state variables of a system. The solidified material is characterized by a certain regular pattern in which the particles are arranged. Recall that for a two dimensional material in the crystalline phase, the arrangement has the form of a triangular lattice.

In the previous chapter we discussed growth of a single droplet surrounded by a liquid phase as an application to the PFC-method. We will now investigate a process which is more likely to occur in nature, that is growth of a polycrystalline material by use of the same method. A simple model of the process is a system in which several individual droplets are surrounded by a uniform liquid. Below a critical temperature, the disordered liquid phase turns dynamically unstable and the droplets start to grow radially outwards with curvature dependent dynamics. Though the individual grains may have the same periodic lattice structure, the orientations of their lattices might distinguish them. Hence, as the individual droplets grow into each other, a network of grains with different orientations is created. Where the grains of different lattice orientations meet, grain boundaries are formed. The misorientation between the grains in the polycrystalline material breaks the symmetry and hence, the grain boundaries act as defects in the system.

In the previous chapter we ensured the crystalline phase by choosing suitable values for density and temperature, and we continue here in the same manner. We create an inital system consisting of randomly distributed crystalline droplets surrounded by a uniform liquid phase. The initial state variables are chosen from the phase diagram depicted in Fig.(3.1), to ensure a metastable liquid phase. Then, as we quench the temperature below its critical value, the crystalline droplets start to grow. Snapshots of the temporal evolution of the density field through the crystallization process is presented Fig.(4.1).
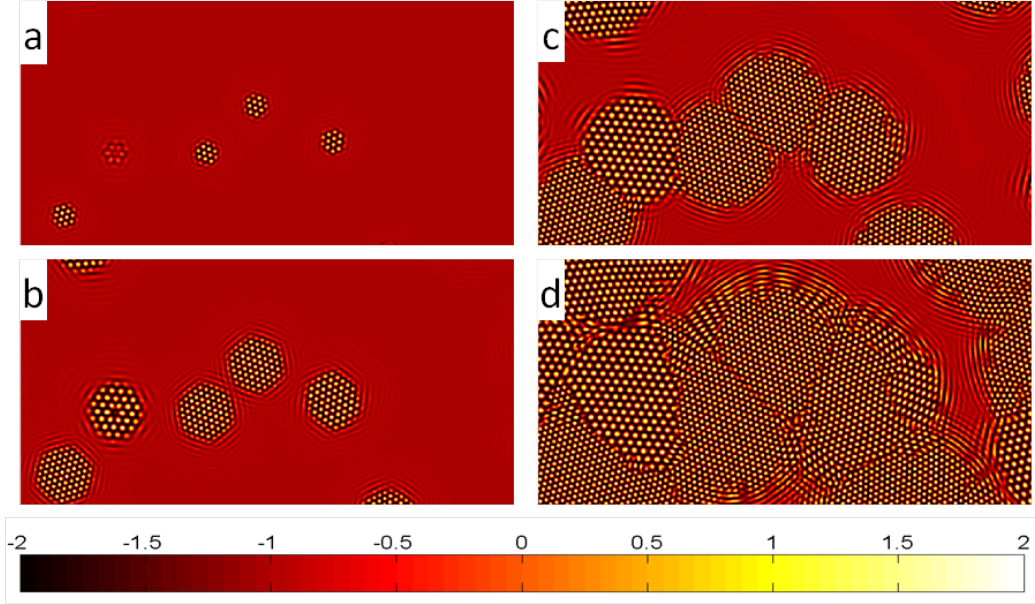
Figure 4.1: (a)-(d) represent snapshots from a numerical simulation of the temporal evolution of growth of a two dimensional polycrystalline material. The inital droplets are randomly distributed and of the same radius. As the individual grains grow they bump into each other and grain boundaries are formed between grains of different orientation. The misorientations lead to symmetry breaking and hence, the grain boundaries act as defects in the system. The pictures are cut outs from a larger numerical simulation with undercooling parameter and mean density, $\alpha = -0.6, \psi_0 = 0.39$, respectively. System size $nx = ny = 1024$

In Fig.(4.1) we see that all the individual grains have density fields with the same periodic structure, but with differently oriented lattices. The average atomic density in the system is relatively constant, [38]. Hence, the periodic density field should vary around an intermediate liquid-phase density. We point out that this is fulfilled in the the density fields depicted in the figure, where the density field within the crystal phase vary from "low" to "high" values, i.e. black to yellow, that is around the density of the liquid phase, the "intermediate" valued red areas.

As the grains grow larger and start to collide, the misorientation between the lattices lead to the formation of grain boundaries and leaves a system simulating a polycrystalline material. The droplets are squeezed together at the grain boundaries, but continue to grow in the directions where they are not hindered by other grains. Hence they loose their close to circular gemometry and regular curvature. The latter is closely related to the growth rate and thus the droplets do not longer grow at the same rate. The combination of changing growth rate and the hinders due to other droplets in the sytem, leaves a network of arbitrarily sized and shaped grains separated by grain boundaries.

The freezing process can also be investigated by means of the evolution of the amplitude fields, represented by the amplitude equations which we discussed in the previous chapter. The pictures presented in Fig.(4.1) are enlarged views of a part of a larger numerical simulation of the liquid-solid transition, and in Fig.(4.2) we present the evolution of the corresponding amplitude field for the whole system.
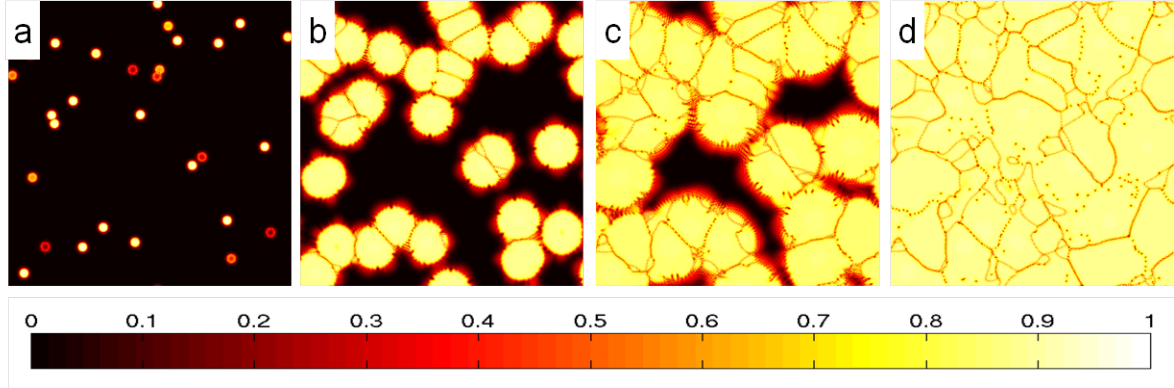

Figure 4.2: Pictures (a)-(d) depict the temporal evolution of the amplitude field of a polycrystalline material through a freezing process induced by a homogenous temperature drop in the system. High values of the field parameter (yellow)indicates crystal phase, low values(black)represent the liquid phase while the intermediate values(red) represent grain boundaries within the polycrystal. Simulations are carried through with undercooling parameter $\alpha = -0.6$ and mean density $\psi_0 = 0.39$. System size $nx = ny = 1024$.

In Fig.(4.2) we present snapshots of the temporal evolution of the amplitude field of a system through the freezing transition. The initial system consists of randomly distributed blobs with crystalline structure which is surrounded by a homogeneous liquid phase. As the homogeneous temperature field in the system suddenly drops below the critical temperature, the blobs start to grow. The periodic structure of the crystalline phase corresponds to high amplitudes and is hence depicted as yellow regions in the system. We point out that the values of the amplitudes are increasing through the freezing process until it saturates to the equilibrium values, that is the brightness of the amplitude fields within the crystalline material is decreasing. Hence, the "strength" of the periodic structure is increasing. Notice also that the growing blobs obtain a six-fold anisotropy at their surfaces, that is there is anisotropy in the system, a tendency that was also noticable in Fig.(4.1). As the blobs grow larger, they create a solid network of grains separated by grain boundaries. Notice now, that the internal grain boundaries in the system are much thinner than the quite sharp boundaries between the liquid phase and the crystalline phase. Even in the fully solidified system, Fig.(4.2(d)), the grain boundaries appears as droplets organized in buckled lines, reminding us of a boundary. Notice also the defects in the system which are not connected in any boundary-like structure.

Both the isolated defects and the grain boundaries, i.e. the misorientation in the material, are energetically costly. That is, their presence in the material is noticable in the free energy functional. Through the phase transition, we notice that these grain boundaries deform slightly as the grains collide and form the polycrystalline network. This deformation contributed to the free energy by means of an elastic energy contribution. In the next section we will discuss the possibility of investigating the state of deformation in the material by means of the elastic energy field.

4.2.1 Elastic energy density fields

As previously discussed, the PFC-method is capable of incorporating the elastic properties of a material. That is, the free energy functional contains a contribution due to deformations in the material through an elastic energy term. Hence, an investigation of the elastic energy field can indicate the state of deformation in a material, and its evolution through a phase transition. In [38], Yeon et al. present a calculation of the linear elastic energy, in the limit of small deformations. Consider a small deformation on the amplitude form, that is $A_j = A e^{i\mathbf{k}_j \cdot \mathbf{u}}$, for each of the modes $j = 1, 2, 3$. This elastic deformation field contributes to the elastic part of the free energy by means of the squared $\mathcal{L}$-operator, that is $\mathcal{L}^2 = (\nabla^2 + 2i\mathbf{k}_j \cdot \nabla)^2$. For the $j = 1$-mode we obtain

$$
\begin{aligned}
|\mathcal{L}_{\mathbf{k}_1} A_1|^2 &= |(\nabla^2 + 2i\mathbf{k}_1 \cdot \nabla) A e^{i\mathbf{k}_1 \cdot \mathbf{u}}|^2 \\
&\approx 4A^2 \left(\mathbf{k}_1 \cdot \nabla(\mathbf{k}_1 \cdot \mathbf{u})\right)^2,
\end{aligned} \tag{4.1}
$$

where the last approximation is valid in the continuum elasticity limit. That is, the limit of elastic behaviour of the material, which is represented by a critical stress at which the deformation field, $\mathbf{u}$, turns permanent. For stresses beyond this elastic limit, the higher order gradient terms are included due to their contribution to the finite elastic deformations. The $\mathbf{k}_j$-vectors are the lattice vectors representing a hexagonal crystal, that is

$$
\mathbf{k}_1 = -\frac{\sqrt{3}}{2}\mathbf{i} - \frac{1}{2}\mathbf{j}, \quad \mathbf{k}_2 = \mathbf{j}, \quad \mathbf{k}_3 = \frac{\sqrt{3}}{2}\mathbf{i} - \frac{1}{2}\mathbf{j}, \tag{4.2}
$$

with $\mathbf{i}$ and $\mathbf{j}$ being the unit vectors in the xy-plane. That is, the elastic energy density contribution to the free energy functional is determined as the sum over the three modes,

$$
E = \sum_{j=1}^{3} |\mathcal{L}_{\mathbf{k}_j} A_j|^2 \approx 4A^2 \sum_{j=1}^{3} \left(\mathbf{k}_j \cdot \nabla(\mathbf{k}_j \cdot \mathbf{u})\right)^2 \tag{4.3}
$$

In Fig. 4.3 we present the elastic energy density field corresponding to the density field depicted in Fig.(4.1d).
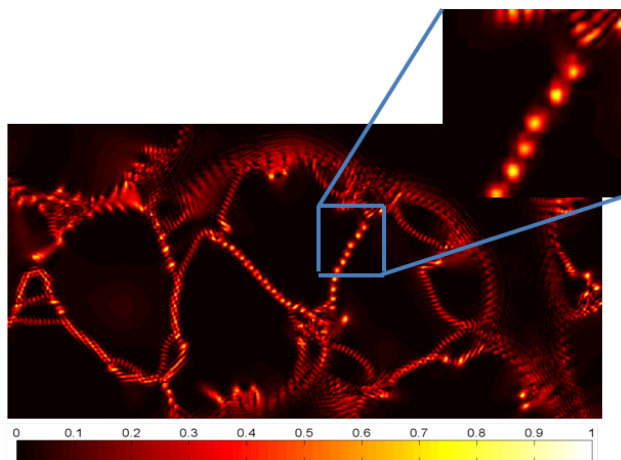
Figure 4.3: The picture depicts an enlarged view of the elastic energy density field of the polycrystalline material during the freezing process and corresponds to the density field represented in Fig. (4.1(d)). The bulk of each grain is in equilibrium and hence there is no deformation in these areas. At the grain boundaries, however, the elastic energy density is higher, that is red areas. The boundary does not appear as uniform along its length and in the inset figure, which is a further enlargement on a part of the grain boundary, it clearly appears pointwise as 'dots' with particularly high energy (yellow core). Cut out from system size $nx = ny = 1024$.

In Fig.(4.3) we see how the elastic energy density changes adruptly across the grain boundaries. The bulks of each grain are in their equilibrium state. Hence there is no deformation within these areas, that is there is no elastic energy density. The grain boundaries are however stretched and deformed as the initially individual grains starts to collide. Notice the tendency, emphasized in the inset figure, that the grain boundaries partly consist of localized regions, in which the energy is higher than in the more uniform parts of the grain boundaries.

In the next section we will focus on the solid-liquid phase transition, i.e. the process of melting. We will discuss some of the aspects which are considered imporant for the melting transition, as well as discuss two of the theories which have been observed experimentally.

4.3   Melting

Liquids can be undercooled and in coexistance with solid surfaces, whereas no crystal can be superheated without loosing its crystallinity. The melting process of a crystalline material is defined as the prosess of reducing the order in the system resulting in a disordered liquid. One of the puzzles is to understand the role of crystalline dimensionality and defects, which most often is present in the lattice structure. The interest in the former originated from the discovery by Peierls that the range of order

in a system is dependent on the dimensionality of the system, hence the breakdown of order is also expected to be dependent on dimensionality [9]. The latter has motivated the development of several theories with melting being mediated by dislocations. One of them is the theory of pair-dislocations unbinding resulting in two successive continuous phase transitions, as described by Kosterlitz, Thouless, Halperin, Nelson and Young (KTHNY) [18, 39, 32]. The competing theory of grain-boundary induced melting, which predicts a preemting of the KTHNY-scenario and causes a single first order transition, was proposed by Chui in Ref. [7].

We will in the following sections discuss the role of dimensionality and dislocations through the melting transition and investigate the two main competing theories of dislocation-mediated melting in two dimensional systems.

4.3.1   The role of dimensionality

While three dimensional crystals generally melt through a first order phase transition associated with a latent heat release, the two dimensional case is not as easy to characterize. Hence, the role of dimensionality is one of the concepts that has been investigated in the search for the fundamental melting mechanism. As mentioned earlier, Peierls proposed theories of melting in lower dimensions based on the effect of the collective behavior of atoms in a structure [9]. At the abosolute zero, all atoms are at rest and the system is motionless. For temperatures above zero Kelvin, the atoms stay relatively fixed in their lattice with only small vibrations around their positions. For increasing temperatures, these vibrations are increasing and the atoms are allowed to be further displaced from their equilibrium positions. The structure of the solid determines the atoms ability to stay in their regular structure. The long range order in the system is kept as long as two atoms situated on a long distance from each other manage to keep their correct relative positions to each other.

Peierls modeled a one dimensional solid as a linear chain of atoms in which the atoms can only sense the position of their nearest neighbours [9]. For temperatures above the absolute zero, the atoms will vibrate around their regular positions in the chain and hence be somewhat displaced from their equilibrium positions. Consider now two long distanced atoms which are connected in a one dimensional chain. Due to the chain structure, which ensures that both atoms have only two nearest neighbours, the atoms have only one path from which they can extract "information" about the position of the other atoms. As all the atoms along this path vibrate around their correct positions, the two long-distanced atoms are not likely to obtain the right relative position. Thus, at finite temperatures, the regular structure is not kept through the array and the long range order in the system is broken.

On the other hand, in three dimensions, the atoms have more nearest neighbours than in the one dimensional chain of atoms. That is, there are more paths between the two long distanced atoms and hence, the atoms can get information about each others positions through these additional paths. Thus they are more likely to maintain

their regular positions despite the increasing vibrational energy in the system. In such three dimensional systems, the long-range-order in the system persists until the temperature in the system reaches the melting temperature of the material. At this well defined melting point, the long-range-order breaks discontinuously and a first order phase transition has occured [9].

The intermediate situation of melting in a two dimensional system is more interesting. The boarderline between the three dimensional long-range-order and the one dimensional disorder, differs from both of the other dimensions with its quasi-long-range-order [8]. That is, through the melting process the order decreases with increasing temperatures, but in a much more gradual way than for 3D systems.

This implies that reduced dimensionality prevents the long-range-order we find in 3D and the order of dimensions may play an important role in the melting mechanism. In 1D long-rang order in the array is actually destroyed as soon as the temperature raises above the absolute zero and thus, the 1D crystal does not really exist.

In addition to the effect of dimensionality, there might be thermal excitations in a system which will influence the energy in the system and hence affect the melting transition. An example of such thermal excitations are defects, such as dislocations, which in nature always will be incorporated in crystalline materials. Hence, the theory of dislocation mediated melting is a common theoretical approach to the melting mechanism.

4.3.2   Dislocation mediated melting

Dislocations are thermal excitations which work as defects in a solid structure. The energies of these thermal excitations increase with increasing temperature and hence change the properties of the solid [8]. The dislocations in a material can be either isolated, bound in pairs or connected in chains, e.g. internal grain boundaries in a polycrystalline material. The theories of dislocation mediated melting are based the interaction between the dislocations in the material. As the interaction potentials between the dislocations contribute to the free energy of the system, [32], the degree of interaction between the dislocations can influence the equilibrium conditions for the system. That is, the density of dislocations and their arrangement in the system might be connected to the state of matter. For low temperatures, all atoms and dislocations are bound. Hence, the system is rigid and has the form of a solid material. When the temperature increases and approaches the critical temperature from below, the behaviour of the system is more complicated and still not fully understood.

Within dislocation mediated melting there are two competing theories. The first scenario is a defect-unbinding theory, the KTHNY-theory [18, 39, 32]. This theory anticipate that the melting transition is caused by formation of dislocation dipoles which decouple close to the melting temperature. The mechanism of melting predicts two successive continuous phase transitions [32]. Another theory is the grain boundary induced melting proposed by Chui in Ref. [7], that predicts a first order, i.e.

discontinuous phase transition, induced by generation of dislocations which pile up into grain boundaries. The main idea in his work was a prediction that the KTHNY-mechanism would be preempted by premelting at these boundaries. When a material is heated to its critical temperature, the material will start to melt from its bulk. When defects, such as impurities and grain boundaries, are present in the material, we can however experience the phenomena of premelting. That is, the material starts to melt from these defects before the material reaches its critical temperature.

The grain-boundary premelting is dependent on the balance between the free energies of the bulk and the interfaces. Whilst the former will favor the crystalline phase for temperatures below the critical temperature of the material, the latter will favor the creation of a liquid-layer along the boundary or around the isolated core before the critical temperature is reached [21]. As the defects in the system is expected to have an impact on the nature of the melting transition, we will in the following section elaborate upon the theories of dislocation-mediated melting in two dimensions.

4.4   Dislocation mediated melting in 2D

The crystal-based theory of melting is described as a breakdown of the crystalline periodicity as a reaction on a rapid change in state variables, e.g. a rapid temperature increase, which leaves a thermodynamically unstable system. The nature of the breakdown process of thin films is still a puzzle as both the continuous and discontinuous melting scenarios have been observed experimentally [22, 33]. As the breakdown process evolves very differently for different order of the phase transition, it is difficult to reveal the universal behaviour of the melting transition in two dimensions.

As previously discussed, the theories of dislocation mediated melting are based on the interaction between the dislocations in a solid material. Hence, density of dislocations in the material and their structure, that is their way of organizing in the material, is expected to be of importance for the nature of dislocation-mediated phase transitions. The KTHNY-theory is based on a physical picture of pairwise interacting dislocatios, dipoles, which interact through logarithmic potentials. The transition theory argues that the energy cost of having isolated dislocations in the system, requires the temperature in the system to be rather high for them to appear. Hence, the dislocation pairs will be tightly bound in pairs as long as the temperature is low, but increasing temperature will allow for the dislocations to be less bound. Thus, the proposed theory describes the melting transition by means of a gradual reduction of the interaction potentials within the dislocation-pairs in the material.

In a low-energy system the dislocations are assumed to appear as tightly bound dislocation-dipoles, interacting through logarithmic interaction potentials. As long as the dipoles are assumed not to interact with other dipoles in the system, they act as isolated dislocations and the logarithmic interaction potential within each dipole is not reduced. In Ref. [18], the authors define a threshold for when the dipoles

are expected to be independent on other dislocation-dipoles. That is, the dipoles in the system moves independently on each other if the ratio between the typical size of the dipoles and the distance between each dipole is kept below this certain threshold. Above this threshold, however, the dipoles are no longer expected to move undisturbed in the system, and the interaction potential within each dipole is reduced through interactions with other dipole-pairs. In order to describe this reduction, Kosterlitz and Thouless drew a parallell between the theory of dislocation interaction and magnetic systems, in which the reduction of interaction potentials within the dislocation-dipoles were described similar to the 'screening-effect' known from the electro magnetic systems [17]. As the melting point is approached from below, the interaction potentials within the dislocation-dipoles are gradually reduced due to the interaction with other dipoles in the system.

The free energy in the system is defined by means of the hamiltonian energy, as a sum of two contributions. That is the energy due to the pairwise interactions and the temperature dependent entropy in the system. As the former reduces and the latter increases for increasing temperature, the entropic contribution the free energy functional will change sign when the energy function changes sign. At this turning point, an instability, defined as the point were the first dislocation-dipole dissociates leaving isolated dislocations in the system, occurs [18]. The gradual dissociation process leads to a gradual change of state, that is a continuous phase transition. The existance of a second continuous phase transition was suggested by Halperin, Nelson and Young after elaboration upon the original ideas of Kosterlitz and Thouless, [32], resulting in the KTHNY-theory of melting. They expected that the KT-instability did not cause a full melting transition, but that it rather led to a transition from the solid phase to an intermediate hexatic phase. That is a phase that has properties between the mobile liquid phase and the rigid solid structure. An additional transition was therefore added to the theory, leading to a theory of melting, the KTHNY-theory, which predicts that two dimensional materials typically melt through two continuous phase transitions. The first transition, known as the KT-instability, is the transition from the initial solid phase to an intermediate hexatic phase and the second from the hexatic phase to an isotropic liquid phase.

The other dislocation-mediated-melting scenario is the grain boundary induced melting process proposed by Chui in Ref. [7]. As previously discussed, grain boundaries are naturally incorporated in polycrystalline materials as boundaries between subgrains of different orientations, that is they take the role of surface defects of each of the grains in the network. A grain boundary is defined to consist of an array of dislocations, [32], and might hence mediate the melting transition for temperatures below the critical temperature of the material. Chui's calculations indicated that a hexatic phase above the critical temperature, as predicted by the KTHNY-theory, does not exist and in Ref. [7], he proposed a theory in which the KTHNY-scenario is preempted by a first order melting transition. In this theory, generation of new dislocations which pile up and create new grain boundaries are expected to occur before

the bulk of the system reaches the melting temperature, T_c. Thus, Chui predicted a first order melting transition for all two dimensional materials.

Later, the theory have been shown to break down for dislocations with core energies above a certain threshold. The core energy is defined as the energy within the area at which the dislocation does not interact logarithmically with other dislocations, that is inside the core radius of the dislocation [32]. That is for defects which have high core energies. Hence the defects are likely to exist in a dilute system. Simulations performed by Strandburg [32], indicate that that the nature of the phase transition changes from the one-step first order transition to a two-step continuous transition as a critial core energy value is approached from below. Above this threshold, the distance between the dislocation pairs become large. Then, the KTHNY-theory for the behaviour of dislocation-dipoles in a dilute medium appears appropriate [32]. Whilst, the KTHNY-theory does not predict any increase in the number of dislocations [39], the grain boundary mechanism is based on the creation of new dislocations which pile up and form internal grain boundaries. Hence, the two theories are quite distinct in their description of the melting transition.

In Ref. [2], Berry et al. present their study of dislocation-mediated melting in three dimensional systems by use of the phase field crystal method. The numerical simulations are performed with bcc-symmetry, which corresponds to the 3D version of the two dimensional triangular lattice. The authors argue that, in the limit of small misorientations between the grains, that is $\theta \to 0$, the dislocations appear as individual "cores" and can by approximation be treated as isolated dislocations. Hence, the melting transition can be investigated by a study of the evolution of the core-size of each dislocation. At the temperature where the initially distinguishable dislocations start to coalesence, the energy of the grain boundary becomes increasingly uniform along its length. That is a liquid-like layer is formed along the grain boundary. Now, the approximation of isolated dislocations does no longer hold, as the energy of each dislocation is expected to decrease due to 'screening' from the other dislocations in the grain boundary [2].

As long as the individual dislocations are distinguishable, it is possible to measure the evolution of their radius as the temperature in the system increases. By quantitative measurements of the radius of melting around the core, we can investigate how much these defects premelt the system before the temperature in the bulk reaches the critical temperature of the material. According to Berry et al. in Ref. [2], a quantitative description can be obtained by means of continuum elasticity theory as long as the grain boundaries are below a certain critical angle, θ. In Ref. [21], Mellenthin et al, present their study of grain-boundary melting through the phase field crystal method. They investigate the evolution of both high- and low-angle boundaries as the melting point is approached from below, and find qualitatively different behaviours for the two cases. Whilst the defects in low-angle boundaries are found to be 'dots' surrounded by a liquid layer, the high-angle boundaries are uniformely wetted along their lengths [21].

Berry et al. investigated the premelting due to dislocations in a three dimensional crystalline material. We will in the following sections perform a similar investigation of the melting transition in two dimensional systems. The phase transitions are triggered by exposing thin films of crystalline materials to a homogeneous temperature increase and applied external load, both separately and in combination.

4.4.1 Melting by temperature

The process of melting can be induced by driving a material out of its equilibrium state by increasing the temperature of a solid material. The polycrystalline material depicted in Fig.(4.2d) provides a fully solidified system and possess a good initial system for investigating of the melting process. In Fig.(4.4) we present the temporal evolution of the melting process, by means of the evolution of the amplitude field, for a polycrystalline material which is exposed to a homogeneous temperature increase.
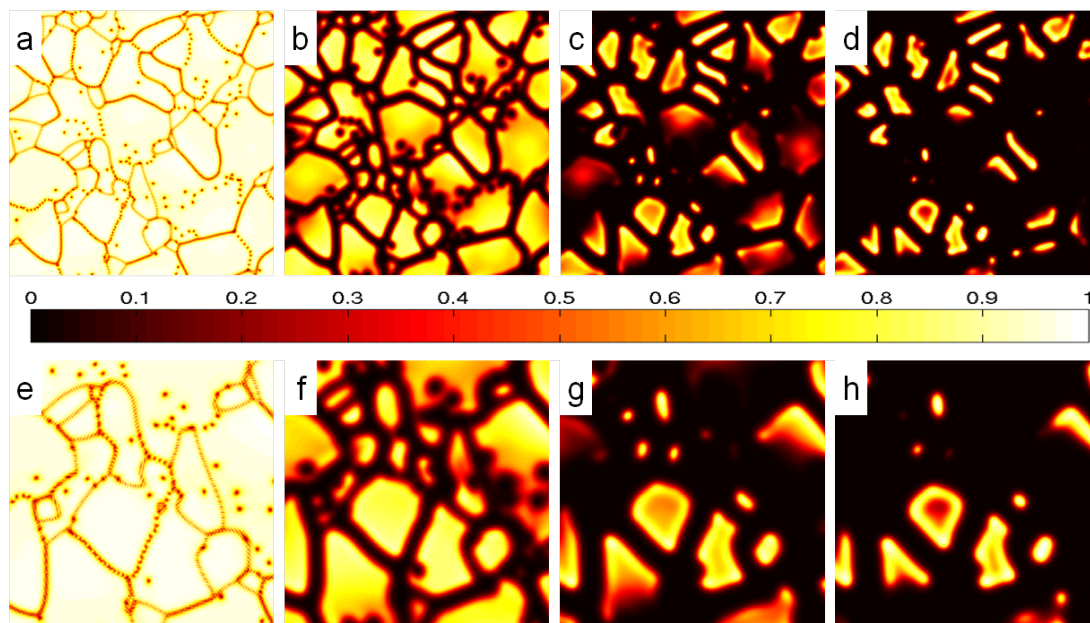

Figure 4.4: Pictures(a)-(d) depict the temporal evolution of the mean amplitude field of a polycrystalline material through a melting transition induced by a homogeneous temperature increase in the system, whilst pictures (e)-(f) depict a zoom-in of a certain area in the same system. High values of the field parameter(yellow) indicate the crystal phase, low values (black) represent the liquid phase whilst the intermediate values(red) represent grain boundaries and other defects in the material. The gradients across the grain boundaries give the cross over from the uniform liquid to the periodic solid. Simulations are carried through with undercooling parameter $\alpha = -0.35$ and mean density $\psi_0 = -0.39$. System size $nx = ny = 1024$.

The temperature increase causes a phase transition through which the polycrystalline material melts and looses its strength, as depicted in Fig.(4.4(a)-(d)). The periodic crystalline structure with density peaks is represented by amplitudes, whilst the density field in the liquid state takes an homogeneous mean value. In the amplitude field, the former is represented by high values, i.e. yellow, whilst the later takes the zero-value, i.e. black. We see that the amplitudes are decreasing through the phase transition, that is the yellow crystalline phase gets brighter, mostly starting from the grain boundaries and moving inwards in the bulk of the individual grains. The grain boundaries in the material grow thicker with time, that is, the solid material is reduced from a fully solidified phase to smaller pieces of solid material surrounded by a liquid phase. The amplitude fields in the individual pieces are non-zero, whilst they are separated by regions of zero-amplitude fields(black regions), that is the liquid phase. Although the general tendency is that the phase transitions seem to originate at the internal surface defects, the grain boundaries, and the additional individual defects, there are however also some tendency of bulk melting at later times.

The pictures in Fig.(4.4(e)-(h)) represent enlarged views of the lower right part of the amplitude field through the transition. We see that the interfaces between the two phases are embossed by gradients in the amplitude field. At early times, the melting is in general focused at the grain boundaries, that is surface melting at each of the grains. As time evolves, we notice a tendency of changes in the amplitude field from the bulk of some of the grains. Notice in particular the single grain situated in the center of Fig.(4.4(g)-(h)). The amplitude field of the grain is decreasing from both its grain boundary its bulk. At the latest picture, we see the tendency of a zero-amplitude field inside the grain, i.e. the tendency of a liquid phase. Notice in particular that there are no defects in the bulk of this crystalline droplet which can induce premelting. Hence the crystalline phase seems to reach its critical temperature before the defects in the system manages to melt the solid material fully. In Fig.(4.5) we present enlarged views of a part of the density field of the crystalline material as it evolves through the melting transition. The pictures represent approximately the same area as the ones depicted in Fig.(4.4(e)-(h)).
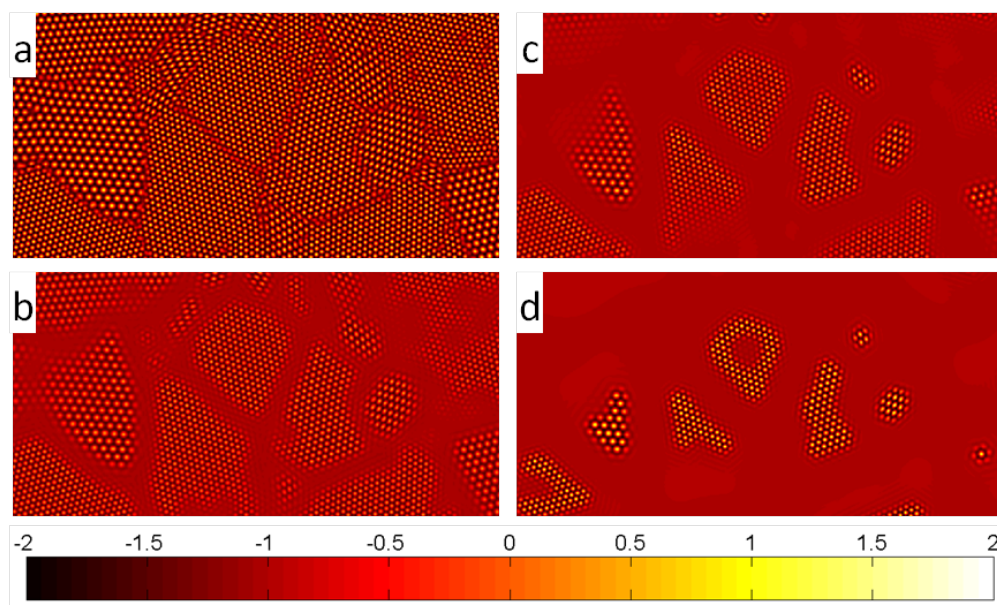
Figure 4.5: (a)-(d) represent snapshots from a numerical simulation of the temporal evolution of a melting two dimensional polycrystalline material. The pictures are enlarged views of a part of a larger numerical simulation, depicted in Fig.(4.4), with state variables in the system, $\alpha = -0.35$ and $\psi_0 = -0.39$. System size $nx = ny = 1024$.

By studying the evolution of the density field, we get a rather good impression of how the crystalline solid is reduced through the phase transition. Notice in particular the grain which we discussed by means of its amplitude field. In Fig.(4.5d) we can see that the crystalline grain have melted from the bulk and left a liquid like phase inside the grain, leaving a doughnut-like structure. Hence, the melting transition seems to initiate from both the bulk and the defects. We emphasize that the enlarged part of the system which we are discussing is not situated at the very boundary of the numerical simulation, hence the external boundaries of the system can not be expected to cause this effect. That is ,the temperature in the bulk reaches the melting temperature before the defects and the grain boundaries cause the grain to melt completely.

The dynamics of the phase transition is dependent on the size of the temperature change, i.e. how far away from the equilibrium state we drive the system. In Fig.(4.6) we illustrate this dependence by presenting a late time step for the melting of the polycrystalline material as it is exposed to homogeneous temperature fields characterized by different α-parameters. For comparison we present both the elastic energy density and the density fields for the four melted polycrystalline materials.
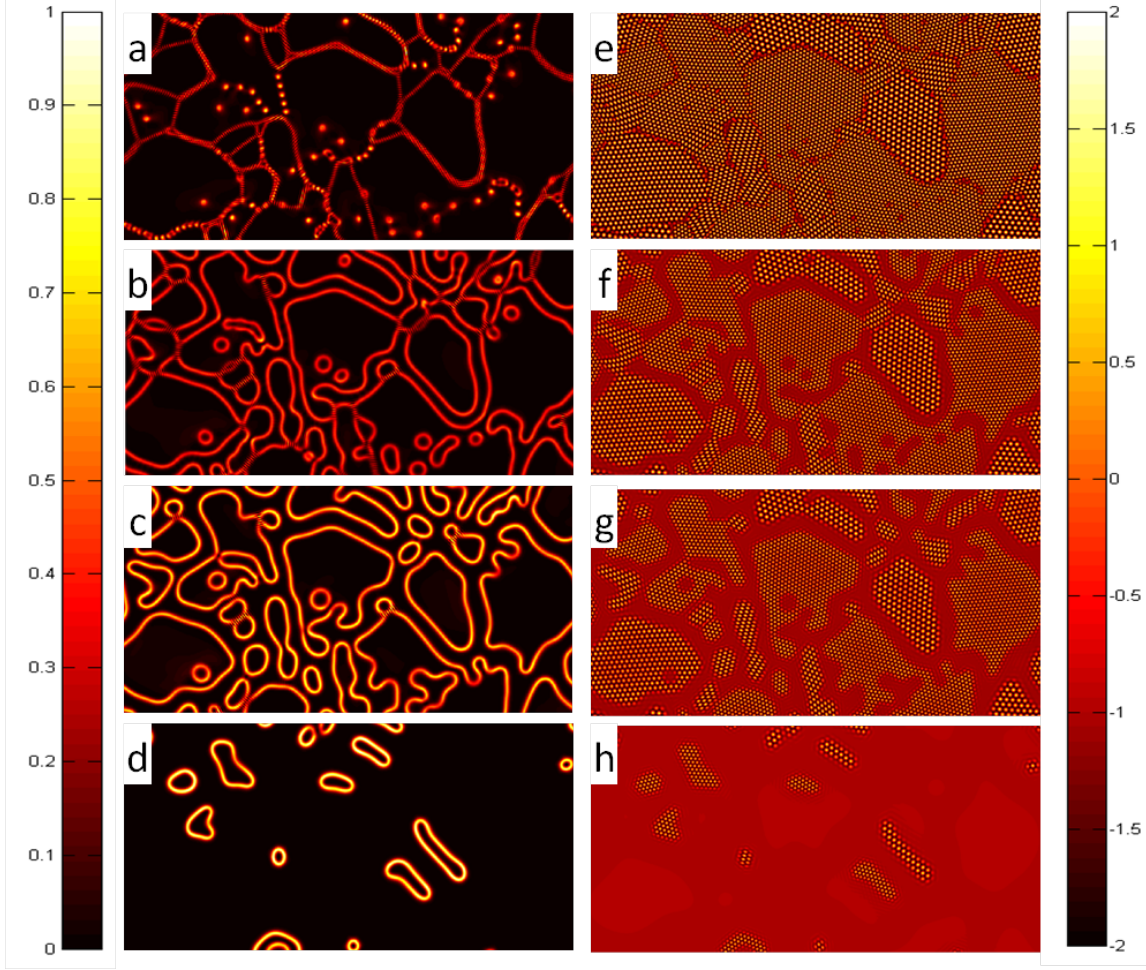
Figure 4.6: Pictures (a)-(d)depict the elastic energy density fields of a polycrystalline material melted at different temperatures, ranged from lower to higher, whilst pictures (e)-(h)depict the corresponding density fields. The pictures give the melted polycrystalline at the same late timestep, but for different values of the undercooling parameter α. (a)-(d) corresponds to $\alpha = -0.5, -0.4, -0.38, -0.35$ respectively. The mean density is fixed at $\psi_0 = -0.39$. System size $nx = ny = 1024$.

The different values of the α-parameters clearly results in different degree of melting for the same late time. The crystalline phase depicted in Fig.(4.6e) is exposed to a homogeneous temperature corresponding to undercooling parameter $\alpha = -0.5$ for a longer period of time, but it still seems to keep its rigid structure. From its elastic energy field, we can also see that the grain boundaries in the system are still well defined. Additionally, there are still individual defects in the system, for which the radius has not increased sufficiently for the melting transition to be noticed. As previously discussed, defects in a material, such as dislocations or grain boundaries, are energetic costly. The pictures in Fig.(4.6(f)-(g)) correspond to temperature pa-

rameters $\alpha = -0.4, -0.38, -0.35$, respectively, at a fixed value of the mean density. That is they are ranged based on the applied temperature fields, from low to higher, and each of the pictures correspond to the same time steps in the phase transition. We point out that the phase transitions for all temperatures leave single crystalline droplets surrounded by a liquid phase, but notice also that the increasing temperature results in higher degree of melting, as expected. The elastic energy density fields for the same phase transitions are depicted in Fig.(4.6(a)-(d)). As previously pointed out, the elastic density field for $\alpha = -0.5$ is embossed by single defects and grain boundaries which are not uniform along its length. For increasing temperatures, we see a tendency of melting from the previously single defects. That is, the radius of the defects are increasing and equilibrium phases are formed within their core and further increasing temperatures seems to enlarge this tendency. Additionaly, the increasing temperature seems to result in wider grain-boundaries, i.e larger elastic energy density.

Back to the single crystals

We have discussed the tendency of polycrystalline materials premelting from their grain boundaries, that is the surface defects of each of the grains making up the polycrystalline material. Even though we in the previous chapter argued that it is not very likely to discover single crystals in nature, an investigation of single crystals melting can give an indication of how the melting transition of a polycrystalline material evolves after the solid network of grains have subdivided into single crystals surrounded by a liquid phase. We will now investigate the melting process of a single crystalline material. Recall the simulation setup for the single crystal growth as discussed in the previous section, that is an inital blob of crystalline material surrounded by a uniform density field, simulating a metastable liquid phase. When we quenched the temperature in the system, the inital blob started to grow. The evolution of the freezing process is depicted in Fig.(3.4), in the previous chapter. We now let the single crystal grow until it spans the whole system size. The fully grown crystal contains impurities, both in its bulk and along the external boundaries of the system. In Fig.(4.7) we compare the melting transition for a single crystal and a polycrystalline material, both being imperfect materials containing defects.
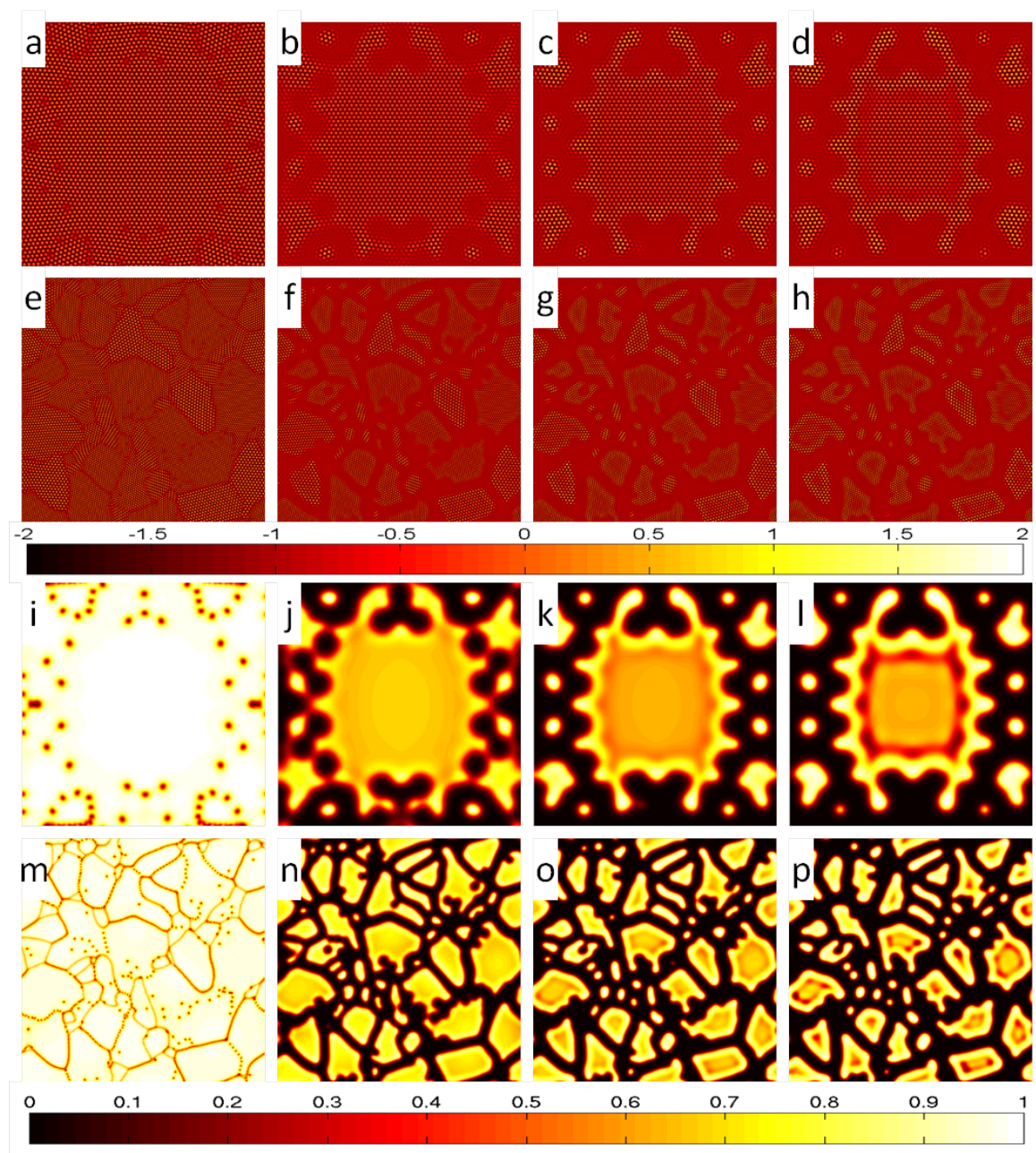
Figure 4.7: Comparison of the melting process for a single crystal and a polycrystalline material. Both systems are exposed to a temperature increase with undercooling parameter $\alpha = -0.36$ and have mean densities $\psi_0 = -0.39$. Pictures (a)-(d) and (e)-(h), illustrate the evolution of the density fields through the phase transition, whilst (i)-(l)and (m)-(p) illustrate the related amplitude fields. System size $nx = ny = 1024$.

From pictures Fig.(4.7(a)-(d)) we see the tendency that the single crystal melts from defects due to the six-fold anisotropy which we also discovered during the process

of single crystal growth in the previous chapter. At a late time, the system consist of a large single crystal surrounded by a liquid phase with some additional smaller "dots" of crystals which have broken off. Comparing the hexagonal anisotropy pattern from the growing crystal in Fig.(3.4) with the melting process depicted in Fig.(4.7(a)-(d)), we see a tendency of melting starting at these anisotropies and move inwards in the bulk of the crystal.

Comparing the evolution of the phase transition for the polycrystalline material and the single crystal, we see a tendency that both the density fields and the amplitude fields of the fully grown single crystals seem to coincide pretty well with each of the single crystals in the partly melted polycrystalline material. We recall the crystalline droplet from Fig.(4.5), which appeard to melt both at the surface and from its bulk, leaving a doughnut-like crystalline phase surrounded by a liquid phase. Fig.(4.7(i)-(l)) illustrates the evolution of the amplitude fields for the single crystalline material through the phase transition. Notice how the crystalline material is affected by impurities even at early times and that the melting transition seems to start at these points and move inwards in the crystal, leaving a system consisting of a large crystalline phase surrounded by a liquid phase and small single crystalline droplets.

In Fig.(4.7(l)) we notice that the amplitude field inside the bulk of the main single crystal is rapidly decreasing. Hence, it seems like the crystal starts to melt from its bulk in addition to the melting initiated by the surface defects and additional anisotropy which we have already discussed. The crystal does not melt fully in its bulk, hence the doughnut like structure from Fig.(4.5) does not appear in this simulation. Remember however that we now investigate the melting transition at a lower temperature, thus we expect the crystal breakdown to develop slower and not reach the same level.

Notice that Fig.(4.7(m)-(p)) illustrates the evolution of the amplitude fields for a melting polycrystalline material, this is equivalent to the process depicted in Fig.(4.4). The two melting processes start from the same initial polycrystalline material, which we produced previously through a freezing process, but the applied temperature field are different in the two cases. Whilst the process depicted in Fig.(4.4) is induced by a temperature field with parameter $\alpha = -0.35$, the temperature field applied in Fig.(4.7(m)-(p)) corresponds to $\alpha = -0.36$. Hence, the latter melting process is carried through in a colder system than the former. For $\alpha = -0.35$ we see that at the last time step, the polycrystalline material is reduced to a system in which a few "dots" of crystalline material are surrounded by a homogeneous liquid, whilst we for $\alpha = -0.36$ see a somewhat slower melting of the polycrystalline material. Except the expected difference due to difference in the degree of heating up the systems, the melting transitions seem to evolve in similar manner. For both phase transitions we see the same tendency of melting starting from the internal defects, both the point defects and the grain boundaries, and that the amplitude fields in the bulks of the crystalline grains starts to decreases at later times. Hence, its seems like impurities in

the material induce premelting of the material before the bulk of the material reaches the critical temperature and starts to break down. In the case of the fully grown single crystal, the purity in the bulk of the crystalline phase was higher and hence, the melting transition left a rather large single crystal surrounded by a liquid phase.

So far, we have investigated the melting transition through exposing both polycrystalline materials and single crystals to a homogeneous temperature increase. According to Khantha et al. in [17], the crystalline material looses its strength the solid is exposed to shear stress. That is, if a material is exposed to both stress and temperature, the material is expected to be weaker and break down earlier. In the next paragraph we will investigate the behaviour of the polycrystalline material when it is exposed to shear stress. We will thereafter combine a homogeneous temperature increase with the applied shear stress to see how the melting transition evolves in loaded systems.

4.4.2 Deformation and stress-assistance

The KT-transition occurs in the limit of zero applied load. In Ref. [17], Khantha et al. argue that a similar transition can occur in systems which are exposed to external stresses. That is a smooth stress-induced generation of new disloations which move around in the system due to the applied load. As previously discussed, a phase transition is expected to occur at the point where the free energy changes sign, that is at the point where the entropic contribution is larger than the enthalpy in the system. The increasing dislocation density reduces the enthalpy in the system and hence, the enthalpy in a loaded material is lower than in a non-loaded material. In addition, the applied shear stress will induce a temperature increase in the material [19]. That is, the combination of the two can trigger a cooperative instability, similar to the KT-instability, that is expected for temperatures close to the critical temperature, to occur in the system without increasing the temperature in the system.

If a material, in addition, is exposed to an increasing temperature, the entropic contribution to the free energy will have an additional increase. Hence, the free energy can change sign even earlier and we can expect premelting at temperatures even further below the critical temperature of the material [17].

As applied load is expected to trigger the creation of new defects in the material, the PFC-method can provide a good tool for description of this process. We notice however, that the temperature increase which is induced by the applied shear stress, is smeared out in the diffusive time scale of the PFC-method. That is, we keep the temperature in the system fixed, though the theory of elasticity predicts an increasing temperature. By use of the same polycrystalline material as we produced in the freezing process, we will now investigate the effect of exposing the system to an external shear flow, both with and without the additional temperature increase. An illustration of the numerical setup and snapshots from the evolution of the amplitude fields through the process is depicted in Fig.(4.8).
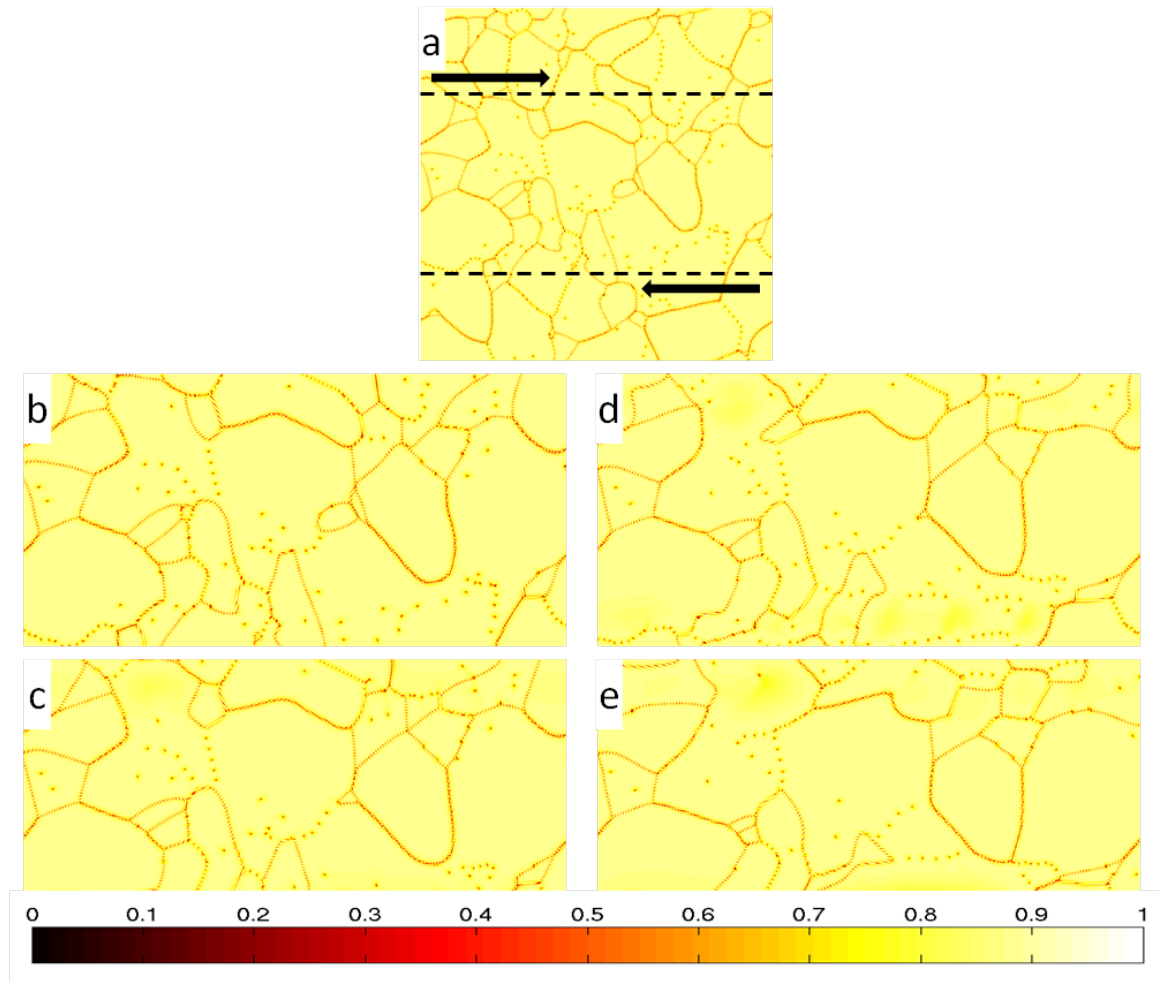
Figure 4.8: Picture (a) illustrates the numerical setup for applying external load to the polycrystalline material. The arrows indicate the direction of the applied shear stress, whilst the dotted lines mark the limited area in which the material is exposed to stress. Pictures(b)-(e)depict snapshots of the temporal evolution of the amplitude field between the dotted lines in (a), as the material is exposed to shear stress. In order to ensure that the evolution in the system is caused by the applied load, the temperature field is set at $\alpha = -0.75$ in the simulation. The inital polycrystalline solid was solidified at $\alpha = -0.6$, hence the system is now kept rather cold. System size,(a), $nx = ny = 1024$.

In Fig.(4.8) we present snapshots from the temporal evolution of the amplitude field for a polycrystalline material which is loaded externally. Due to the periodic boundary conditions in the system, the shear stress is applied in the bulk of the solid material in order to avoid the shear stress to add up at the boundaries. Hence, we can control that the polycrystalline material is exposed to the same amount of load for the whole simulation. During the evolution, we see that the individual grains in

the polycrystalline network deform. Some grains disappear in the transition, whilst others are created. The shear stress causes the dislocations to move around in the system and there seems to be a tendency for them to move towards the already existing grain boundaries in the system. There is however an additional tendency of creation of new defects in the material, that is in regions of somewhat lower amplitudes which we recognize by brighter yellow colour. The decrease in the amplitude field indicates that the periodic structure of the crystalline phase is reduced, and hence appears as weaker. This is consistent with the theory, which predicts generation of dislocations when a material is weakened by external loads. As the tendency of dislocation formation is not very clear in Fig.(4.8), we present an enlarged view of a part of the system at some successive time steps of particular interest in Fig.(4.9).
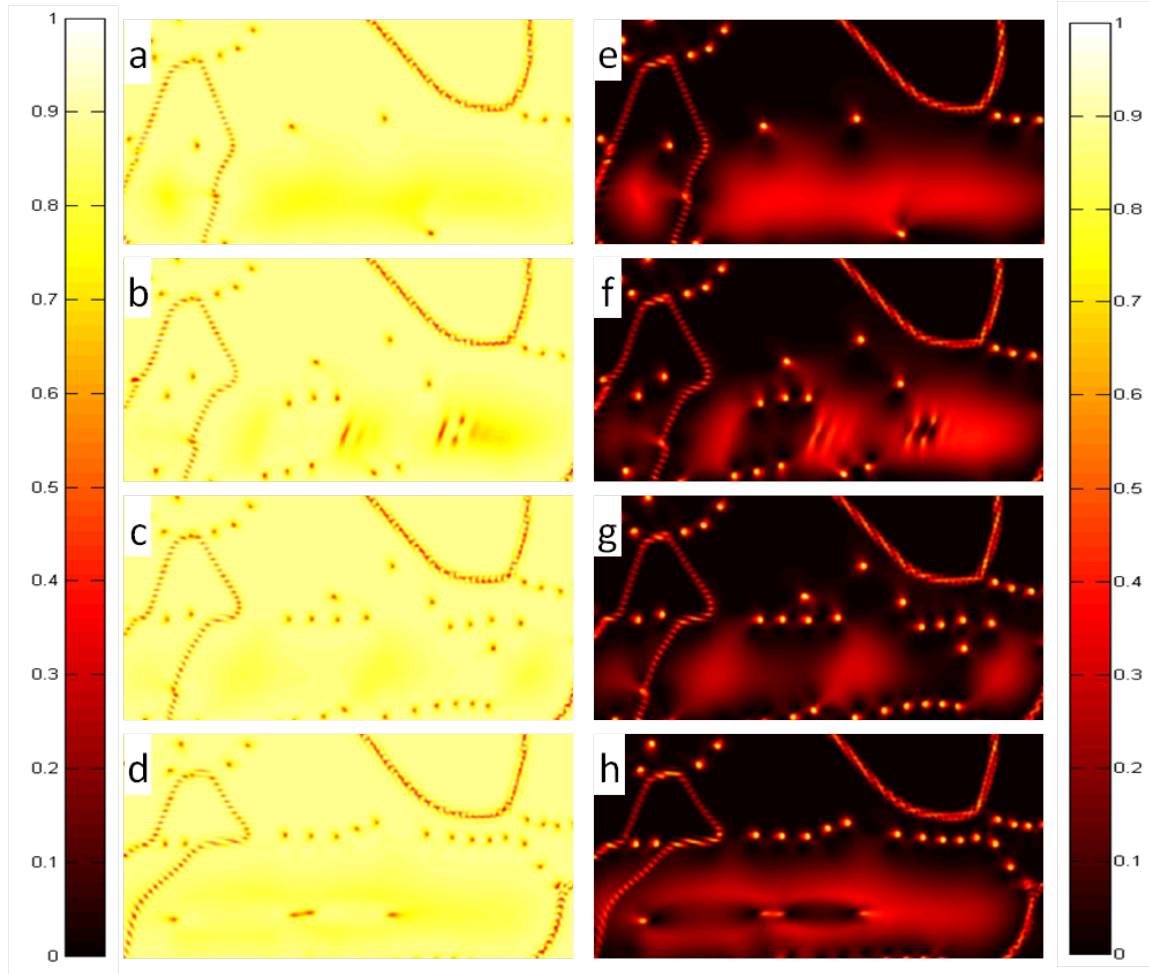
Figure 4.9: Pictures (a)-(d) illustrate enlarged views of a part of particular interest in the amplitude field of a polycrystalline material as it is exposed to shear stress. The pictures correspond to the same evolution process as depicted in Fig.(4.8), but for different time steps. Pictures (e)-(h) depict the elastic energy density fields corresponding to the amplitude fields (a)-(d). Undercooling parameter $\alpha = -0.75$. Out cut of system size $nx = ny = 1024$.

In Fig.(4.9) we present the amplitude fields and energy density fields of a certain area of the simulation for a short time period in which interesting phenomena appear. In the first picture, (4.9(a)), we count three independent defects in the middle of the material and we notice the tendency of a brighter yellow region, which indicates decreasing amplitudes in the periodic structure, in the lower part. A few timestep later, that is Fig.(4.9(b)), the number of dislocations have increased, appearing in the lower, bright yellow region where the periodic crystalline structure is weaker. The defects have a tendency to form as elongated red areas which thereafter separate into two fairly circular shaped defects. This might correspond to nucleation of dislocation

dipoles which later unbinds and go separate ways due to local shears. In the lower part of the pictures, that is close to where the shear stress is applied, the newly created defects start to move. In the next snapshot, that is Fig.(4.9(c)), we see that no more defects are created. We notice, however, that the defects start to gather closer to each other, moving towards the centre of the area. Notice in addition that two of the three initial defects from Fig.(4.9(a)) is still situated somewhat in their original positions. This suggests that the shear stress which was applied at the lower boundary has not yet propagated through this area. This can also explain why the new defects in the material seem to be generated only in this area. In Fig.(4.9(d)) we see two interesting phenomena. The first is that both the initial and the newly created defects are starting to pile of to create a new grain boundary in the material. The second is that a new process of defect generation has started in the lower region of the area. We notice also that the grain on the very left side of the area has deformed through the evolution and that new defects have been created also in the centre of this grain. The creation of new defects seems to occur in the bulk of each grain, that is in the areas which are farthest away from the grain boundaries. Fig.(4.9(e)-(h)) illustrates the corresponding elastic energy density fields. In the previous elastic density fields which we have presented, the bulk areas of each grain have been in the equilibrium state. As the material now is loaded, the bulks are slightly deformed and will there will be an elastic contribution to the free energy functional. In the simulations, we observe the predicted increasing deformation through the increasing elastic energy within the bulks of the grains. We notice, however, that this only occurs in the bulk areas close to where the shear flow is applied. This implies that the lower parts are more deformed, which is a clear indication that the effect of the shear flow has not yet propagated up through the material. The generation of defects appear only in the areas of increasing elastic energy density, that corresponds to the areas where the amplitude fields are decreasing. Notice that when the defects are generated as elongated areas of higher energy, they appear with significantly lower energy than the isloated defects after the separation process.

So far, we have studied the polycrystalline material by means of two protocols, that is applied load and homogeneous temperature increase, separately. Through the former we observed that the applied shear stress triggered the creation of new defects, whilst the latter indicated melting transition being induced by defects in the solid material, though without increasing the dislocation density. Hence, we would expect the combination of the two protocols to accelerate the melting process, as discussed by Khantha et al. in Ref. [17]. We will in the next section elaborate more upon the stress-assisted melting transition.

4.4.3   Stress-assisted melting

We have previously discussed premelting and formation of wet layers around the defects for increasing temperatures. The presence of such liquid films at the grain boundaries can reduce the resistance to shear stresses, [21]. Thus premelting around the defects can weaken the heated materials and make them more sensitive to applied shear stress.

In Fig.(4.10) snapshots from the evolution of a polycrystalline material as it is exposed to both a homogeneous temperature increase and applied shear stress.
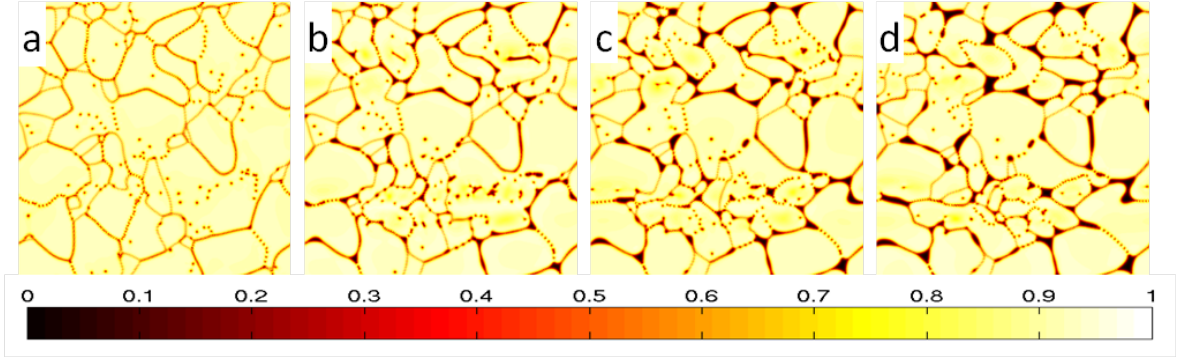

Figure 4.10: Pictures(a)-(d)depict snapshots of the temporal evolution of the amplitude field of a polycrystalline material is it exposed to both a homogeneous temperature increase and applied shear stress. Undercooling parameter $\alpha = -0.5$ and mean density $\psi_0 = -0.39$. System size $nx = ny = 1024$.

The simulation depicted in Fig.(4.10) is carried through with undercooling parameter $\alpha = -0.5$. Though this temperature increase is relatively small compared to the parameter of the melting process presented in Fig.(4.4), we can clearly see that the crystalline structure in the material breaks down, typically by creation of wet layers along the uniform grain boundaries. Hence, it seems like the applied shear stress reduces the material strength and causes the material to melt at lower temperatures, as discussed in Ref. [17].

In order to investigate this possible reduction of material strength, we present comparisons of the amplitude and elastic energy density fields for the different protocols at late times, that is close to their relaxed state, in Fig.(4.11). Pictures (a)-(f) illustrates the two protocols separately as well as in combination.
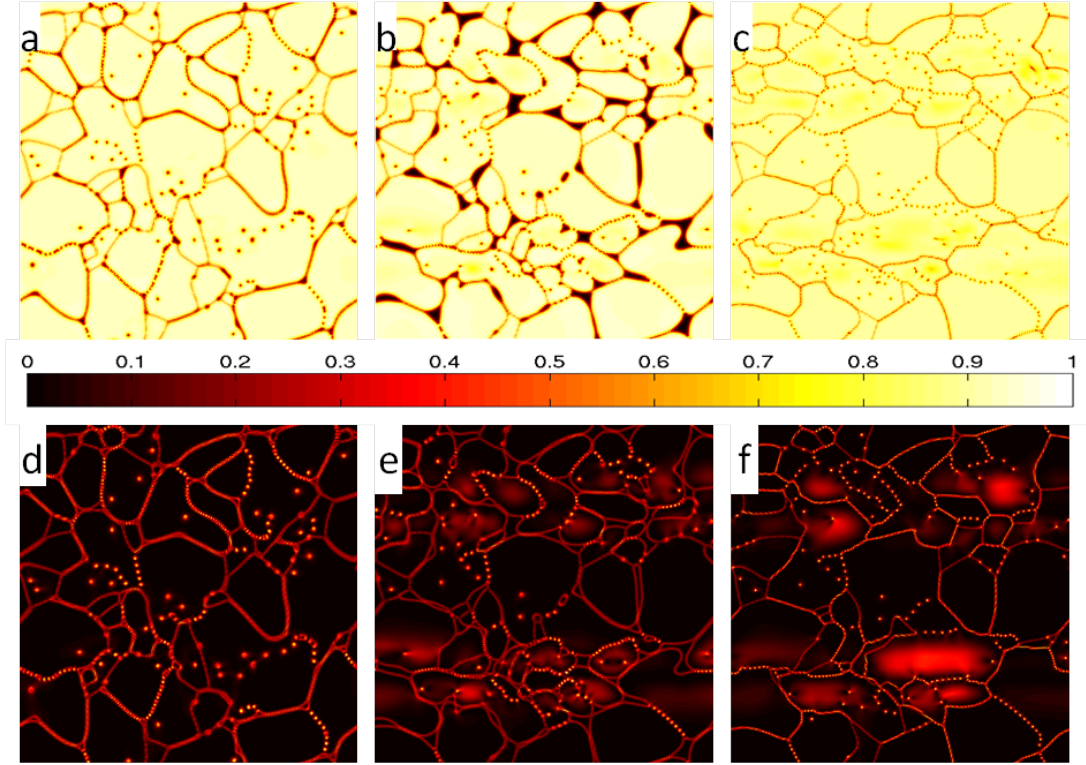
Figure 4.11: Pictures (a)-(c) and (d)-(f) depict comparisons of the amplitude and elastic energy density fields, respectively, at late times for a polycrystalline material which is exposed to a homogeneous temperature increase and shear stress. Picture(a) and (d) depict the fields after a homogeneous temperature increase corresponding to $\alpha = -0.5$. (c)and (f) illustrate the fields of a material which is exposed to shear stress at cold temperature, $\alpha = -0.75$. The intermediate pictures, (b) and (e), represent a late time snapshot of a melting transition induced by a combination of the two protocols, with $\alpha = -0.5$. The mean density is fixed at $\psi_0 = -0.39$. System sizes $nx = ny = 1024$.

Fig.(4.11) depicts the amplitude fields and the corresponding elastic energy fields of a polycrystalline material close to its relaxed state after it has been exposed to,(a) and (d), a homogeneous temperature increase, (c)and (f) applied load in terms of an external shear flow and (b) and (e), a combination of the two protocols. As previously discussed, the density of dislocations in a material is expected to increase when a system is exposed to external stresses. We notice that the number of individual defects in Fig.(4.11(c)) is significantly larger than in the two other systems. In this situation, however, the material still seems rigid, that is, the system seems to still be fully solidified. There is no clear sign of melting from the defects, but we notice that the amplitude fields are brighter, that is the amplitudes seem to be some what reduced even though the system seems to keep its rigidity. In Fig.(4.11(b)) we see the expected tendency of a further developed melting transition in a loaded

system. The dislocations that enumerate and pile up as grain boundaries at the same time as they induce melting in the system, leaving a system that is partly melted, even for low temperatures $\alpha = -0.5$. The individual grains in the network are still connected, but dark regions in the amplitude field implies that there is liquid present in the system. The corresponding elastic energy density fields, Fig.(4.11(d)-(f)),underline the tendency we pointed out for the amplitude fields. We can however see the tendency of deformed grains more clearly in these pictures. We point out Fig.(4.11(e)) and the areas where the shear stress is applied. The grains in these areas are typically smaller than in both the rest of the area as well as in the other pictures in the figure. In addition, the number of dislocations in this area seems to be higher than in both the two other systems. This implies that the material looses its resistance to temperature increase when it is exposed to shear stress, as predicted by theory [17]. We emphasize that the homogeneous temperature increase, $\alpha = -0.5$, was chosen in a way that ensured that the melting transition was not carried through before the applied stress managed to propagate in the system and start the creation of new dislocations.

In the nest section we will give a brief overview of some of the experiments that have been carried out in order to figure out whether the melting scenario occurs in accordance with the KTHNY-theory, or if it is preempted by the grain-boundary melting-scenario.

4.5   Experimental work

Both the KTHNY- and the grain-boundary-scenario have been observed in experimental work in different systems [22, 33]. Hence, it has been difficult to argue that either of them provides a satisfactory description of the melting transition in two dimensions. To reveal the characteristic features of the melting scenario in two dimensional systems, various experimental investigations have been performed. Even though the experimental techniques have improved greatly the last years, they have still not been successful in revealing the order of the observed melting transitions and hence obtaining a full understanding of the melting mechanism. In Ref. [40], Zahn et al. present their analyze of a two dimensional melting process in a system of colloidal particles, and argue that their results support the two-stage melting transition with an intermediate hexatic phase. Hence, their results indicate that the KTHNY-theory provides a basis for decribing the melting transition in two dimensions. A contradictary result is presented in Ref. [22], that is experimental work performed by Nosenko et al. in two dimensional complex plasma systems. The authors compare their results with both the two-step continuous phase transition and the one-step first order scenarios, and argue that their results suggest that the KTHNY-scenario is preempted by the grain-boundary induced melting mechanism for this system.

Similar experimental work has been carried through in order to investigate the order of the freezing process. In Ref. [10], Dillmann et al. present their investigation

of crystallization in a two dimensional colloidal system. The motive of the experiment was to adress the question of whether the hexatic phase occurs in the system upon cooling. As they quench an initial isotropic liquid phase, small crystallities starts to grow in the system. After some time, they grow into each other creating a polycrystalline material. This experiment is hence similar to our numerical study of the freezing process. Dillmann et al. argue that there is no indication of the hexatic phase through the temperature driven crystallization process. Hence, the process of freezing seems to be first order.

In this chapter we have discussed liquid-solid phase transitions, that is the processes of freezing and melting. We have discussed the two models of particular relevance, being the KTHNY- and grain-boundary induced melting scenarios. The former represents two continuous phase transitions and the latter a single first order phase transition. We have presented our numerical results of freezing and melting, and discussed our results upon the two competing scenarios. Additionaly, we have given a brief introduction to a small piece of the experimental work that has been performed, motivated by the wish to understand the melting mechanism.

Chapter 5

Discussion

In the previous chapter we presented numerical results from our study of the liquid-solid phase transition, i.e. freezing and melting, in two dimensions. We focused especially on the latter and evaluated our results upon the most relevant theories of dislocation mediated melting. The melting transition was studied with a homogeneous temperature increase, as well as with reduced material strength by means of applying external shear stress. We thereafter performed a comparison of melting transitions induced by these two protocols. In this chapter, we will summarize our results and compare them to studies of similar systems performed by others, that is both numerical and experimental investigations. As a final word, we will discuss ideas for future work as well as point out some of the challenges that remain in the search for a general theory of the mechanism of two dimensional melting.

To determine the order of the melting transition in two dimension is perhaps the biggest struggle in the search for the melting mechanism. The abrupt nature of the first order transition predicted by Chui in Ref. [7], leaves no sign of the intermediate hexatic phase that is predicted in the theory of the two continuous melting transitions described in the KTHNY-theory, [18, 39]. The puzzle which remains is that both the scenarios, despite their very different nature, have been observed experimentally. Whilst Zahn et al. in Ref. [40] present their results indicating a continuous phase transition in a system of colloidal particles, experiments performed by Nosenko et al., [22] suggest a first order transition induced by grain boundaries in their study of two dimensional complex plasmas. Hence, the unresolved question is which physical conditions that leads to either of the scenarios.

5.1 Core energy and dislocation density

Within the theory of disocation mediated melting, the evolution of the melting mechanism is assumed to be dependent on the core energy of the dislocations in the material. Recall that the core energy is defined as the energy within the area where the dislocation does not interact logarithmically with other dislocations, that is inside the

core radius of the dislocation [32]. In Ref. [30], Saito argues that both the KTHNY-scenario and the theory of grain boundary induced melting are possible, dependent on the typical core energy of the dislocations in the material. Though Strandburg, in Ref. [32], questions the validity of his simulated first order transition, his results are rather tractable as he argues that whilst high core energies cause the dislocation unbinding mechanism, low values of the core energy will cause a preempting of the continuous phase transition. Chui, [7], argues however that the phase transition will be first order, irrespectable of the core energy. He distinguishes between weak and strong first order, at a certain threshold, the same threshold as others, Ref. [32], define at the threshold between the first order and the continuous phase transition scenarios. Hence, from a theoretical point of view, the mechanism of melting in two dimensions seems to be somewhat understood.

That is, an estimation of the core energy for the dislocations in a material might reveal the nature of the melting transition. To estimate this value is however not a simple task, neither by numerical simulations or through experiments. As prevoiusly discussed, the defects in the material can be isolated, coupled in pairs as well as contained in grain boundaries. Hence, in areas of high dislocation density, such as in grain boundaries, it is not necessarily possible to separate the defects from each other. Whilst the dislocations are still separable in some grain boundaries, recall the grain boundary depicted in Fig. 4.3, other grain boundaries are uniform along their length. Previously we discussed the energy reduction due to screening which occurs when dislocations interact with each other [32]. As the core energy is the energy of a dislocation can not be reduced, the screening effect will not affect the energy we want to measure. Though it is difficult to measure the core energy for isolated dislocations, it is even more difficult when we can not distinguish them from each other. The problem of determining the core energy of a dislocation is also a difficult task from the experimental point of view. It would involve measurements of thermodynamical quantities at a microscopic level. Experimentally, such measurements are very difficult to perform, [32, 21].

A second criterion which can be useful in the study of the two theories are their distinct predictions of the evolution of the dislocation density. Whilst the grain boundary induced melting transition predicts generation of new dislocations through the phase transition, the KTHNY-scenario of continuous phase transitions predicts a constant dislocation density. Hence, a quantitative investigation of the number of dislocations in the material through the transition can reveal the nature of the phase transition, i.e. its order. Such an investigation is possible through numerical simulations. In our simulations, the defects in the material are clearly visable and can hence be counted by use of numerical techniques. Though we have not specified whether the observed defects are single dislocations or other types of defects, we expect that an increasing number of defects in throughout the simulation would indicate an increasing number of dislocations in the material, implying a first order melting transition by means of theory of grain boundary induced melting.

An additional discussion involves the different kinds of defects that is assumed to occur in the system. The continuous phase transitions in the KTHNY-theory, are defined as dissociation of defects of different types. Hence, the possibility of distinguishing between various types of defects is beneficiary in the work of developing a further understanding of the melting mechanism. In Ref. [30], Saito argues upon a criterion which determines whether the melting transition is continuous or of first order. Saito does however only include dislocations in his model and hence, he can only investigate the KT-transition and the dissociation of dislocation-dipoles, and not the second transition in the full KTHNY-theory [32]. We emphasize however that his work was published in 1982 and that the evolution within computational techniques have developed to a very great extent since then. According to Tegze et al. in Ref. [33], the various attempts to investigate the two phase transitions in the KTHNY-theory have led to diverse results. Whilst some investigations indicate that the first transition is continuous and the second of first order, others suggest that it is the other way around. In Ref. [33], Tegze et al. present their numerical investigation of freezing and melting, through the phase field crystal method. They do not observe any hexatic phase in their simulations, but claim that the lack of an intermediate phase might be caused by limitations of the phase field crystal method. That is the possibility of the time averaging in the PFC-model smearing out the information regarding the structure in the hexatic phase and hence make the model unable to distinguish the fluid phase from the hexatic phase.

5.2   Phase transitions in geological systems

Mineralogy is an area of Earth science which treats the structure and stability of minerals[26], that is the behaviour of the minerals on Earth and how they respond when the geological environment which they are situated in changes through geological processes. Melting and recrystallization of minerals are of specific interest as it is well known that the high temperature, and pressure, differences between the Earth's surface and its interior cause incessant transitions between solid rocks and viscous magma. The mineralogical side of the geoscience is embossed by these phase transitions and has improved a lot after taking condensed matter physics into account [16, 29].

Rocks are polycrystalline materials consisting of grains of different minerals. The different minerals have different chemical composition and hence different melting temperatures. That is, if the rock is exposed to a temperature increase, some of the minerals might melt whilst others remain solids. This phenomenon is known as partial melting and results in a system of both melt and solid. As the solid minerals are less bound along the resulting liquid-solid interface, elements from the mineral composition might dissolve into the fluid and change the composition of both the solid mineral and the melt.

If the temperature decreases and the melt leaves the system, the recrystallized

material can now consist of different minerals than the original rock. Hence, for geological systems, phase transitions can have an impact on both the crystal structure and the chemical composition. Due to its simple chemical composition, the study of ice is simpler than the study of rocks. The individual grains in ice are all solidified water, and hence changing environmental conditions cannot induce chemical reactions and successive changes in composition. Additionally, all grains in the network have the same melting temperature and are hence only distinguished by their size and lattice orientation.

Though the mechanism of melting is not fully understood, geologists have achieved increasing understanding through laboratory experiments. A record of critical melting temperatures for rocks was obtained through experimental work by means of heating various igneous rocks, that is rocks formed by crystallization of magma [3]. The microstructures of minerals can be investigated through experimental methods. An old and common method is use of polarization microscopy to investigate thin sections of the interesting material. In Fig.(5.1) we present our simulated two dimensional polycrystalline material together with thin sections of ice and rock under polarized light during laboratory experiments.
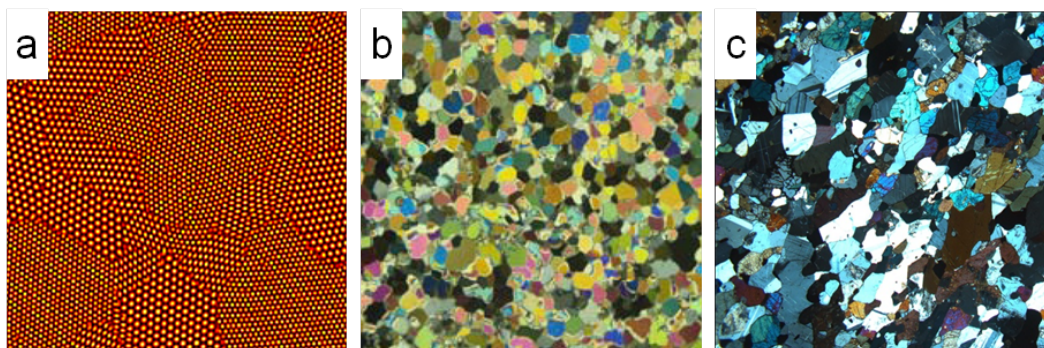

Figure 5.1: (a) snapshot of the crystal density of a polycrystalline material simulated by the PFC-method, shows a material consisting of grains with different lattice orientations (b) thin section (1mm) of ice core sampled during field work in the Barents Sea (1.75 m depth) under polarized light shows differently oriented crystals in a polycrystalline formation (c) optical photomicrograph under crossed polars of a granulite containing quartz, feldspar and pyroxene grains with different orienations. The image was obtained from a standard thin ($30\mu m$) section.

5.3   Summary and future work

The periodic structure in the crystalline phase gives rise to several physical phenomena of interest, e.g. impurities, multiple grain orientations as well as elastic and plastic deformations, [27], all of which are assumed to be important for the evolution of phase

transitions. Information regarding these phenomena is naturally incorporated in the phase field, $\psi(\mathbf{r}, t)$, in the phase field crystal method. In this thesis, we have used this method to investigate the liquid-solid phase transitions numerically. The presented results indicate that the temperature induced melting transition is embossed by melting from the defects in the material, that is both isolated and chain-structured defects.

The defects will influence the mechanical properties of a material [19]. Hence, both the density of them and their behaviour through a phase transition is of importance for the strength of the material. Inspired by this, we have also investigated stress-assisted melting transitions, i.e, melting of materials after having reduced the material strength by externally applied load. We observed, through our simulations, that the combination of applied load and increased temperatures led the melting further, as compared to the melting process in the limit of zero applied stress. That is, the material started to melt before the critical temperature was reached in both the stress-assisted systems and in systems in the limit of zero applied stress. As previously discussed, a quantitative description of the dislocation density as well as measurements of the core energies can be helpful in the investigations of the melting mechanism. Hence, it would be interesting to obtain a qualitative description of the numerical results presented in this thesis. To obtain the additional measure of the core energies within the defects would be very beneficiary in order test the predicted threshold, but this task is more challenging than the counting of dislocations.

The processes of pattern formation and crystalline breakdown can be quite complicated, due to impacts such as anisotropy in the material, chemical reactions as well as deformation due to external forces. If we can determine the conditions for when a phase transition is first order or continuous, we would be a step closer to obtain an understanding of the melting mechanism. Of particularly interest is prediction of the melting temperature, that is the critical point at which a material looses its strength and yields. As the two continuous phase transitions in the KTHNY-theory are associated with different types of defects, a full investigation of this transition would require a model which distinguishes between dislocations and other defects, as well as between isolated dislocations and the ones which are coupled in dipoles.

In order to obtain a better understanding of these phenomena it is necessary to reveal the key processes and variables which triggers the transformation, as well as the physical framework which is capable of predicting their behaviour.

Appendix

Discretization Schemes
Both the spatial uniform density fields and the periodic density fields, the latter with their pertaining amplitude fields, are space and time dependent. All simulations have been carried through with the same discretization schemes.

Spatial discretization

In the numerical simulations we discretize the lattice structure by means of the spherical laplacian as described in Ref. [24, 34]. Ooni et al. argue, in Ref. [24], that for conserved fields the discretization scheme have to contain the contributions from the next nearest neighbours in addition to the nearest neighbour, in order to create an isotropic model. A suitable discretization scheme is hence spherical,
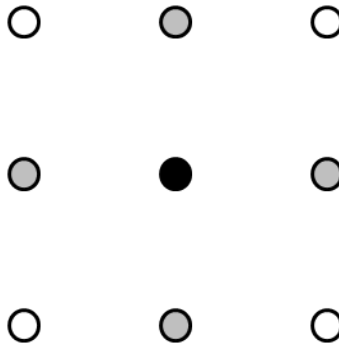

Figure 5.2: Spherical discretization scheme. The black dot represents the considered node. The grey and white dots represent its nearest and next nearest neighbours respectively. The two types of neighbours are weighted differently in the discretization scheme.

The gradients in the lattice structure are discretized as follows, here illustrated with the phase field parameter, ψ,

$$\nabla\psi = \frac{1}{4dx}\sum_{nn}\psi + \frac{1}{8dx}\sum_{nnn}\psi, \tag{5.1}$$

where nn denotes the nearest neighbours, whilst nnn denotes the next nearest neighbours.

The Laplacian acting on the fields is discretized in a similar manner,

$$\nabla^2 \psi = \frac{1}{2(dx)^2} \sum_{nn} \psi + \frac{1}{4(dx)^2} \sum_{nnn} \psi - \frac{3\psi}{dx^2}. \tag{5.2}$$

Amplitude fields

When the differential operator $(\nabla^2 + 1)$ acts upon the amplitude fields, it is denoted by $\mathcal{L}_j = (\nabla^2 + 2i\mathbf{k}_j \cdot \nabla)$

The discretized operator is hence represented by

$$\mathcal{L}_j = \nabla^2 + 2i \left(k_j(1)\nabla_x + k_j(2)\nabla_y \right), \tag{5.3}$$

where $k(1)$ and $k(2)$ denotes the first and second element in each of the hexagonal lattice vectors, k_1, k_2, k_3. and ∇^2 given in Eq. 5.2.

In the numerical simulations we have increased the numerical efficiency by disregarding the differential operator in the prefactor $(1 - \mathcal{L}_j)$ in Eq. 3.33. This leaves a numerical efficient calculation of the evolution of the amplitude field for each of the modes

$$\partial A_1 = \mathcal{L}_1^2 - 3A_1 \left(\alpha - 3\bar{\psi}^2 + |A_1|^2 + 2|A_2|^2 + 2|A_3|^2 + 6\bar{\psi}A_2^* A_3^* \right). \tag{5.4}$$

In addition to the evolution of the amplitude fields, we calculate the evolution of the mean density field. The equation of motion for the mean density is given in Eq. 3.32.

Time discretization

Together with the spatial discretization we apply the forward Euler scheme,

$$\begin{aligned} dA &= \frac{A^{(t+1)} - A^{(t)}}{dt} \\ A^{(t+1)} &= A^{(t)} + dt \cdot dA. \end{aligned} \tag{5.5}$$

We know that is scheme can be unstable, but ensure small numerical error by a choosing sufficiently small time steps, $dt = 0.03$.

We save the mean density fields and the amplitude fields for all time steps and analyse them seperately.

Phase field modeling

Although Oono et al. in Ref. [24] argue that the contributions from the next nearest neighbours are not necessary in system of non-conserved parameters, we have performed all simulations with the discretization scheme described in the previous chapter.

Ginzberg-Landau, Cahn-Hilliard, Swift-Hohenburg and PFC:

- Numerical parameters GL: $nx = ny = 500; dx = 1; dt = 0.01$

- Numerical parameters CH: $nx = ny = 500; dx = 1; dt = 0.001$

- Numerical parameters SH: $nx = ny = 500; dx = 1; dt = 0.001$

- Numerical parameters PFC: $nx = ny = 500; dx = 1; dt = 0.001$

- Physical parameters GL: $\alpha = -1, \psi_0 = 0$

- Physical parameters GL droplet growth $\alpha = -0.25$ and $\psi_0 = 0.25$

- Physical parameters CH: $\alpha = -1, \psi_0 = 0$

- Physical parameters SH: $\alpha = -0.25, \psi_0 = 0.25$

- Physical parameters PFC: $\alpha = -0.25, \psi_0 = 0.25$

- Physical parameters PFC droplet growth $\alpha = -0.25$ and $\psi_0 = 0.25$

PFC with amplitude equations
Freezing
We start out by constructing an initial system consisting of randomly distributed droplets in the bulk. The restriction on the distribution is included in order to avoid droplets at the boundaries of the system. We define each of the initial droplets as solids, that is each of them is represented by periodic fields with different lattice orientations. The system is exposed to a rapid homogeneous temperature drop, controlled by the α-parameter.

For growth of a single crystal, the initial system is simplified to consist of only one inital droplet with periodic structure.

Heating
The initial polycrystalline material is contructed by a reconstruction of the crystal density from the last time step of the freezing process. The process of melting is induced by a homogeneous temperature increase,controlled through by the α-parameter. The melting process is investigated for various values of the α, and the evolution of the amplitude fields and mean density fields are saved for analysis.

For melting of a single crystal, the initial system is constructed by uploading a fully grown single crystal, i.e. an inital single crystal which have grown to fill the entire system size.

Shearing

The code used for investigation of the processes of freezing and melting is modified to apply a stress field to the fully grown crystal. The shear flow is applied at a distance $nx/4$ from the top and bottom system boundaries. This in order to avoid that the shear stress adds up at the boundary due to the periodic boundary conditions. The shear stress is implemented as band of shear velocity, defined across the vertical direction of the system.

The applied shear stress contributes to the spatial evolution of the mean density and amplitude fields by an additional term. This is accounted for through additional gradient fields of each of the amplitude fields as well as for the mean density field, here represented by means of one of the amplitude modes,

$$A_1^{n+1} = A_1^n + dt * dA_1 - dt \cdot v \nabla A_1, \tag{5.6}$$

where v denoted the velocity of the applied field.

Numerical and physical parameters

- Numerical parameters : $nx = ny = 1024; dx = \pi/4; dt = 0.03$

- Figure 3.6 : $\alpha = -0.6; \psi_0 = 0.39$

- Figure 3.7 : $\alpha = -0.6; \psi_0 = 0.39$

- Figure 4.1 : $\alpha = -0.6; \psi_0 = 0.39$

- Figure 4.2 : $\alpha = -0.6; \psi_0 = 0.39$

- Figure 4.3 : $\alpha = -0.6; \psi_0 = 0.39$

- Figure 4.4 : $\alpha = -0.35; \psi_0 = -0.39$

- Figure 4.5 : $\alpha = -0.35; \psi_0 = -0.39$

- Figure 4.6 : $\alpha = -0.5, -0.4, -0.38, -0.35; \psi_0 = 0.39$

- Figure 4.7 : $\alpha = -0.36; \psi_0 = -0.39$

- Figure 4.8 : $\alpha = -0.75$ shear velocity $= 0.05$

- Figure 4.9 : $\alpha = -0.75$ shear velocity $= 0.05$

- Figure 4.10 : $\alpha = -0.5; \psi_0 = -0.39$

- Figure 4.11 : $\alpha = -0.5, -0.75; \psi_0 = -0.39$ shear velocity $= 0.05$

Bibliography

[1] B.P. Athreya, N. Goldenfeld, and J.A. Dantzig. Renormalization-group theory for the phase-field crystal equation. *Physical Review E*, 74(1):11601, 2006.

[2] J. Berry, KR Elder, and M. Grant. Melting at dislocations and grain boundaries: A phase field crystal study. *Physical Review B*, 77(22):224114, 2008.

[3] N.L. Bowen and O.F. Tuttle. The system mgosio2h2o. *Geological Society of America Bulletin*, 60(3):439, 1949.

[4] R.S. Brumbaugh. *The philosophers of Greece*. State Univ of New York Pr, 1981.

[5] J.W. Cahn. Free energy of a nonuniform system. II. Thermodynamic basis. *The Journal of Chemical Physics*, 30:1121, 1959.

[6] JW Cahn and JE Hilliard. Free energy of a nonuniform system. I. Interface free energy. *J. Chem. Phys*, 28(2):258–267, 1958.

[7] ST Chui. Grain-boundary theory of melting in two dimensions. *Physical Review B*, 28(1):178–194, 1983.

[8] JG Dash. History of the search for continuous melting. *Reviews of Modern Physics*, 71(5):1737–1743, 1999.

[9] JG Dash. Melting from one to two to three dimensions. *Contemporary Physics*, 43(6):427–436, 2002.

[10] P. Dillmann, G. Maret, and P. Keim. Polycrystalline solidification in a quenched 2d colloidal system. *Journal of Physics: Condensed Matter*, 20:404216, 2008.

[11] KR Elder and M. Grant. Modeling elastic and plastic deformations in non-equilibrium processing using phase field crystals. *Arxiv preprint cond-mat/0306681*, 2003.

[12] KR Elder, M. Katakowski, M. Haataja, and M. Grant. Modeling elasticity in crystal growth. *Physical review letters*, 88(24):245701, 2002.

[13] KR Elder, N. Provatas, J. Berry, P. Stefanovic, and M. Grant. Phase-field crystal modeling and classical density functional theory of freezing. *Physical Review B*, 75(6):64107, 2007.

[14] FC Frank. Melting as a disorder phenomenon. *Proceedings of the Royal Society of London. Series A, Mathematical and Physical Sciences*, 170(941):182–189, 1939.

[15] N. Goldenfeld, B.P. Athreya, and J.A. Dantzig. Renormalization group approach to multiscale modelling in materials science. *Journal of statistical physics*, 125(5):1015–1023, 2006.

[16] J. Grotzinger and T. Jordan. *Understanding Earth Lecture Notebook*. WH Freeman & Co, 2007.

[17] M. Khantha and V. Vitek. Mechanism of yielding in dislocation-free crystals at finite temperatures–Part I. Theory. *Acta Materialia*, 45(11):4675–4686, 1997.

[18] J.M. Kosterlitz and D.J. Thouless. Ordering, metastability and phase transitions in two-dimensional systems. *Journal of Physics C: Solid State Physics*, 6:1181, 1973.

[19] L.D. Landau, E.M. Lifshitz, JB Sykes, WH Reid, and E.H. Dill. Theory of elasticity: Vol. 7 of course of theoretical physics. *Physics Today*, 13:44, 1960.

[20] H. Lwen. Melting, freezing and colloidal suspensions. *Physics Reports*, 237(5):249–324, 1994.

[21] J. Mellenthin, A. Karma, and M. Plapp. Phase-field crystal study of grain-boundary premelting. *Physical Review B*, 78(18):184110, 2008.

[22] V. Nosenko, SK Zhdanov, AV Ivlev, CA Knapek, and GE Morfill. 2D Melting of Plasma Crystals: Equilibrium and Nonequilibrium Regimes. *Physical review letters*, 103(1):15001, 2009.

[23] A. Ōnuki. *Phase transition dynamics*. Cambridge Univ Pr, 2002.

[24] Y. Oono and S. Puri. Study of phase-separation dynamics by use of cell dynamical systems. i. modeling. *Physical Review A*, 38(1):434, 1988.

[25] D.W. Oxtoby. New perspectives on freezing and melting. 1990.

[26] J.P. Poirier. *Introduction to the Physics of the Earth's Interior*. Cambridge Univ Pr, 2000.

[27] N. Provatas, JA Dantzig, B. Athreya, P. Chan, P. Stefanovic, N. Goldenfeld, and KR Elder. Using the phase-field crystal method in the multi-scale modeling of microstructure evolution. *JOM Journal of the Minerals, Metals and Materials Society*, 59(7):83–90, 2007.

[28] S. Puri. Kinetics of phase transitions. *Phase Transitions*, 77(5):407–431, 2004.

[29] A. Putnis. *Introduction to mineral sciences*. Cambridge Univ Pr, 1992.

[30] Y. Saito. Melting of dislocation vector systems in two dimensions. *Physical Review Letters*, 48(16):1114–1117, 1982.

[31] I. Singer-Loginova and HM Singer. The phase field technique for modeling multiphase materials. *Reports on Progress in Physics*, 71:106501, 2008.

[32] K.J. Strandburg. Two-dimensional melting. *Reviews of modern physics*, 60(1):161, 1988.

[33] G. Tegze, L. Gránásy, G.I. Tóth, J.F. Douglas, and T. Pusztai. Tuning the structure of non-equilibrium soft materials by varying the thermodynamic driving force for crystal ordering. *Soft Matter*, 2010.

[34] H. Tomita. Preservation of isotropy at the mesoscopic stage of phase separation processes. *Progress of theoretical physics*, 85:47–56, 1991.

[35] S. Van Teeffelen, R. Backofen, A. Voigt, and H. L
”owen. Derivation of the phase-field-crystal model for colloidal solidification. *Physical Review E*, 79(5):051404, 2009.

[36] AA Wheeler, BT Murray, and RJ Schaefer. Computation of dendrites using a phase field model. *Physica D: Nonlinear Phenomena*, 66(1-2):243–262, 1993.

[37] J.M. Yeomans. *Statistical mechanics of phase transitions*. Oxford University Press, USA, 1992.

[38] D.H. Yeon, Z.F. Huang, KR Elder, and K. Thornton. Density-amplitude formulation of the phase-field crystal model for two-phase coexistence in two and three dimensions. *Philosophical Magazine, 90*, 1(4):237–263, 2010.

[39] AP Young. Melting and the vector Coulomb gas in two dimensions. *Physical Review B*, 19(4):1855–1866, 1979.

[40] K. Zahn and G. Maret. Dynamic criteria for melting in two dimensions. *Physical Review Letters*, 85(17):3656–3659, 2000.